



Hydrogeochemical Processes and Trace Metal Contamination in Groundwater: Impact on Human Health in the Maputaland Coastal Aquifer, South Africa

Philisiwe P. Mthembu¹ · Vetrimurugan Elumalai¹ · K. Brindha² · Peiyue Li³

Received: 17 April 2020 / Revised: 23 June 2020 / Accepted: 3 July 2020 / Published online: 10 July 2020
© Springer Nature B.V. 2020

Abstract

The main objective of the study is to evaluate the hydrogeochemical processes and potential health risk assessment for humans in groundwater of Maputaland coastal aquifer, South Africa. In this study, 53 and 42 groundwater samples were collected from bore wells during 2018 and 2019 and were analysed for major ions, minor ions, nutrients and trace metals. Na–Cl water type was dominant in groundwater followed by Ca–HCO₃. Cross plots revealed that ion exchange, reverse ion exchange, silicate weathering, seawater mixing and anthropogenic inputs from agricultural activities govern the groundwater chemistry. GIS methods were adopted to produce spatial distribution maps of major ions through which locations of groundwater contamination and the intensity of hydrogeochemical processes were identified. Mean concentration of trace metals were in the order: Zn > Li > Al > Fe > Mn > Cu > Pb > As > Co > Cd in 2018, Fe > Zn > Mn > Sr > B > Pb > Cu > Co > Cr > Cd > Ag > Al > Ni in 2019. Most of the trace metals were found to be within the WHO standards for drinking water except Cd, Zn, Pb, Mn, Al and Fe. Health risk assessment of trace metals in groundwater via ingestion and dermal absorption pathways were carried out. Hazard Quotients (HQs) and Hazard Index (HI) of all trace metals were below 1, except HQ_{ingestion} and HI for Co and Pb which were greater than 1 in children. This suggests that these metals pose adverse risks to local people, and children were more sensitive to risks than adults. HI values for adults and children were medium indicating high risk. This is the first baseline study conducted in the study area which identifies the chemical characterization and the potential health risk due to trace metals contamination.

Keywords Hydrogeochemical processes · Trace metals · Multivariate statistical · Silicate weathering · Health risk assessment

Introduction

Contamination of coastal aquifers is a global concern. Coastal aquifers are mostly affected by salinization due to seawater intrusion (Askri et al. 2016; Bouzourra et al. 2015; Eissa et al. 2016; Vetrimurugan et al. 2017a). Anthropogenic

pollution such as agricultural return flow, disposal of domestic and industrial wastes, etc., also influences the quality of groundwater (Vhonani et al. 2018). Assessment of groundwater chemistry is essential in determining the sources for the composition of ions and to determine its suitability for various uses. Several hydrogeochemical processes occurring beneath the surface can be natural (e.g. rock-water interaction, evaporation, dissolution of minerals, hydrology) and/or anthropogenic (e.g. industry, agriculture, mining, and urbanization) (Das et al. 2016; Di Curzio et al. 2017; Etikala et al. 2019; Ghesquière et al. 2015) and influence the groundwater chemistry. These hydrogeochemical processes tend to vary temporally and spatially.

Trace metals occur naturally in groundwater in minor amounts and are required for human metabolism as well as for growth of the plants and animals. However, the concentration of these metals above the desired limit is known

✉ Vetrimurugan Elumalai
vetrimurugan@yahoo.co.in; ElumalaiV@unizulu.ac.za

¹ Department of Hydrology, University of Zululand, Kwa-Dlangezwa, Richards Bay 3886, South Africa

² Hydrogeology Working Group, Institute of Geological Sciences, Freie Universität Berlin, Malteserstraße 74–100, 12249 Berlin, Germany

³ School of Water and Environment, Chang'an University, No. 126 Yanta Road, Xi'an 710054, Shaanxi, China

to have toxic effects on human health (Jahanshahi and Zare 2015; Tamasi and Cini 2004; Wagh et al. 2018; Yousaf et al. 2016). Elevated Pb concentrations are known to have adverse effects in children during brain development (Tay and Hayford 2016). Long-term intake of high concentrations of Fe through drinking water may cause kidney, cardiovascular, and liver damage (Usman et al. 2020). Exposure to Cd causes acute and chronic diseases such as kidney and skeletal damages (Soleimani et al. 2020). Trace metals are reported to be one of the critical contaminants that affect groundwater quality and pose concern to human health as they are persistent, non-biodegradable, stable and toxic in the natural environment (Tay and Hayford 2016; Soleimani et al. 2020). Trace metals in groundwater are influenced by weathering of rocks, atmospheric deposition and anthropogenic activities (He and Li 2020). The solubility of trace metal is controlled by pH, the content of the trace metal, chemical composition, organic carbon content, and ion exchange (Di Curzio et al. 2017; McMahon and Chapelle 2008; Palmucci et al. 2016).

Health risk assessment is a process of estimating health effects that may occur from exposure to non-carcinogenic and carcinogenic chemicals (Duggal et al. 2017; Zhou et al. 2016). The U.S. Environmental Protection Agency (USEPA 2004) proposed a four-step method for health risk assessment (hazard identification, exposure assessment, dose–response assessment, and risk characterization). It is necessary to assess the risk to human health due to groundwater contamination as there may still be possible health hazards, even if the chemical composition of groundwater is consistent with the drinking water standards (Ji et al. 2020). Several researchers have carried out health risk evaluations to determine the impact of contaminant toxicity on humans (Zhou et al. 2020; He et al. 2020; Egbueri 2020; Egbueri and Mgbenu 2020; Edokpayi et al. 2018; Wu et al. 2019, 2020). Previous studies have reported that children are more exposed to non-carcinogenic risk due to ingestion of groundwater contaminated with trace metals as compared to adults (Barzegar et al. 2018b; Ukah et al. 2019; Zhang et al. 2018; Wang et al. 2018).

South Africa receives an annual average precipitation of approximately 497 mm which is below the world average of 860 mm (Smakhtin et al. 2001). It is a semi-arid country with scarce water resources (Smithers et al. 2017). Rainfall in South Africa is spatially and temporally dynamic (Ndlovu and Demlie 2016, 2018). About two-thirds of the population of South Africa rely on groundwater for water supply. Development on surface and groundwater management is still needed to compensate the shortage of water supply in rural areas (Du Plessis 2017). The country faces numerous water quality issues (e.g. salinization, eutrophication, microbiological contamination, sedimentation, silt migration and acidification) (DWA 2002). Groundwater contamination

by trace metals is often reported in South Africa. Verlicchi and Grillini (2020) reported that arsenic and lead occur in elevated contents in groundwater of South Africa. Demlie et al. (2014) stated that the high iron content in groundwater significantly affects the water supply in the region.

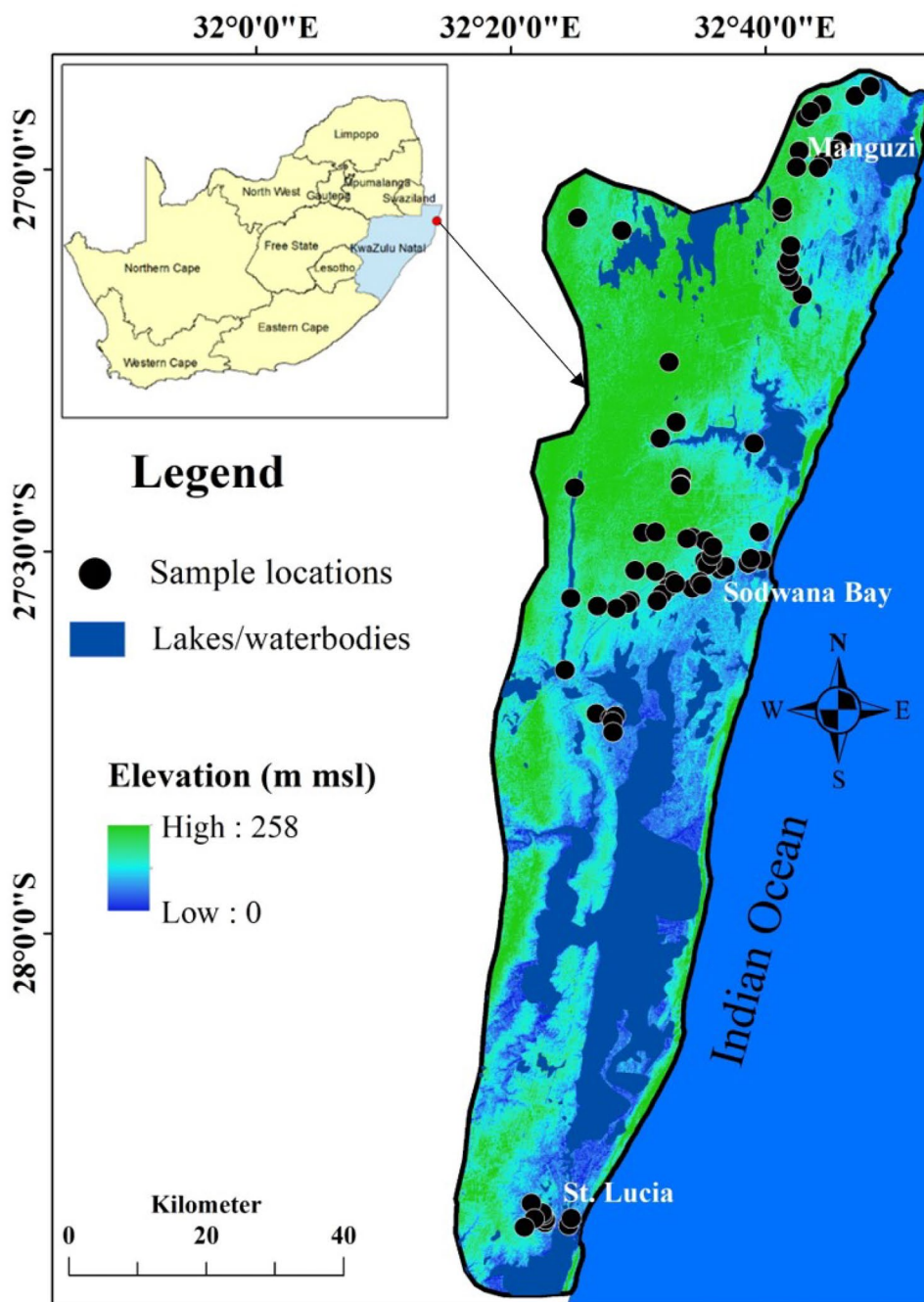
The Maputaland coastal plain is the largest primary aquifer in South Africa (Fig. 1). This coastal plain extends from Mtunzini in the south up to the Mozambique border. Groundwater remains the sole supplier of water for drinking, domestic and agricultural purposes in rural communities in north-eastern KwaZulu-Natal. The availability of groundwater on the Maputaland coastal plain is reduced due to various land use activities including agriculture, livestock farming and forestry plantation. Studies on the Lake Sibayi (Nsubuga et al. 2019; Smithers et al. 2017; Weitz and Demlie 2014) and the impact of land use (Grundling et al. 2013) in the Maputaland coastal plain has been reported. Earlier groundwater studies in the region include identification of sources of iron in groundwater (Demlie et al. 2014), relation between sediment mineral composition and groundwater quality, and groundwater modelling to predict the groundwater levels during dry and wet periods (Kelbe et al. 2016). The hydrogeological processes that control the groundwater chemistry and health risk assessment have not been studied in detail of the study region. Hence, the present study was carried out with the main objectives to (1) evaluate the hydrogeochemical processes, (2) identify the intended sources of groundwater contamination and (3) comprehensive understanding of trace metal contamination and health risk assessment of groundwater using geostatistical and geographic information system (GIS) methods. This study will produce the baseline dataset that could be useful for further systematic investigation and it would also be useful to the department of water affairs, stakeholders and policymakers involved in the water management sector to understand the underlying aquifer conditions to prevent the health hazards from ingesting groundwater, and to effectively perform further development, protection and management of groundwater resources in the Maputaland coastal aquifer.

Methodology

Description of the Study Area

Maputaland coastal plain is situated in north-eastern KwaZulu-Natal province, South Africa (Fig. 1). It is bounded in the west by the Lebombo mountain range, in the east by the Indian ocean, in the north by the Mozambique border and extends up to Mtunzini in the south. It is characterized by humid subtropical climate. Majority of the precipitation in the area occurs during summer and is derived from tropical and mid-latitude weather systems (Smithers et al.

Fig. 1 Location of the study area



2017). Rainfall in the Maputland coastal plain varies spatially, it ranges from approximately 1000 mm/year in the coastal areas to less than 600 mm/year in inland (Porat and Botha 2008; Watkeys et al. 1993). Average annual temperature ranges from 21 °C along the Lebombo mountains to 23 °C inland and to about 22 °C along the coast (Mkhwanazi 2010). This region is of great importance as it is known for its tourism and ecological diversity. Most of the areas are under conservation by the Isimangaliso wetland park.

Geological Setting

The Maputland coastal plain is characterized by a sequence of sediments which overlie the consolidated volcanic rhyolites of the Lebombo group. The geology of the study area comprises of Cretaceous to Quaternary deposits of the Maputland Group that is underlain by the Zululand group. The Zululand group consists of conglomerates and basaltic rocks of the Msunduze, Mpilo and Movene formations. There are also alluvial, fluvial and marine sediments of the

Makatini formation, shallow and marine silts and sands of the Mzinene formation (Watkeys et al. 1993). Karst-weathered calcarenites are found in the Uloa formation which is rich in fossiliferous sediments (Kelbe et al. 2016; Watkeys et al. 1993). The Zululand group are characterized by very low permeability with groundwater of poor quality and quantity. This group comprises of loosely consolidated sand, silts, clays and lignite beds of the Port Dunford formation (Demlie et al. 2014; Meyer et al. 2001; Ndlovu 2015). Grey unconsolidated sands are identified in the Kosi Bay and KwaMbonambi formations. The high coastal dune cordons of the Sibayi formation are highly rich in heavy minerals and are heavily vegetated (Nweze 2016; Watkeys et al. 1993). Sediments of the Maputaland group is characterized by high hydraulic conductivities which averages to 15.6, 0.87, and 4.3 m/day for the Sibayi, KwaMbonambi and Port Dunford formations (Ndlovu and Demlie 2018).

Water Sampling and Analysis

Groundwater samples were collected from borewells within the Maputaland coastal plain in April 2018 ($N=53$) and May 2019 ($N=42$) (Fig. 1). Samples were collected after five minutes of pumping the borewells in order to remove stagnant water. Water from the sampling well was used to rinse the sample bottles thrice prior to sample collection. The pH and electrical conductivity (EC) of the groundwater samples were measured in the field using a calibrated Aqua Probe A-700 m. Three sets of samples were collected in each sampling point, raw samples were collected in 500 ml bottles and the other samples were collected in 200 ml high-density polyethylene bottles, filtered in the field using 0.45 μm Milipore membrane filter. Samples were acidified with 0.5 ml concentrated nitric acid to prevent precipitation of cations and trace metals. CO_3 and HCO_3 were analysed from the 500 ml sampling bottles immediately using standard titration methods (APHA 2012). Collected groundwater samples were analysed for cations (Ca, Mg, Na and K), anions (Cl, SO_4 , F), nutrients (NO_3 , PO_4 , NH_4) and SiO_2 using ion chromatograph (Metrohm 930 IC Compact Flex). A total of fifteen trace metal concentrations (As, Ag, Fe, Mn, Al, B, Zn, Pb, Ni, Cr, Cu, Cd, Co, Li and Sr) were analysed by inductively coupled plasma-mass spectrometry (NexION 2000 ICP-MS). Ten trace metals including As, Fe, Mn, Al, Zn, Pb, Cu, Cd, Co and Li were analysed in 2018 while 13 metals such as Ag, Fe, Mn, Al, B, Zn, Pb, Ni, Cr, Cu, Cd, Co and Sr were analysed in 2019. The ion balance error was calculated to check data quality, is within $\pm 5\%$. To ensure the precision of the chemical analysis of trace metals, the standards and blanks were regularly applied to check the accuracy of the instrument and to avoid errors.

Multivariate statistical analysis has been widely used by various researchers and has proven to be useful in reducing

large dataset to understand the relationships between variables and their contribution to groundwater problems which is to be investigated.

Health Risk Assessment

Health risk assessment estimates health effects that may occur from exposure to non-carcinogenic and carcinogenic chemicals (Duggal et al. 2017; Zhou et al. 2016, 2020; Ji et al. 2020). Human exposure risk of an individual to trace metals in the water occurs in three pathways; direct ingestion, inhalation and dermal absorption through exposure skin (Zeng et al. 2015; Duggal et al. 2017). The doses received through ingestion and dermal absorption pathway were computed using Eqs. 1 and 2 adopted from USEPA (2004)

$$\text{ADD}_{\text{ingestion}} = \frac{C_w \times \text{IR} \times \text{EF} \times \text{ED}}{\text{BW} \times \text{AT}} \quad (1)$$

$$\text{ADD}_{\text{dermal}} = \frac{C_w \times \text{SA} \times K_p \times \text{ET} \times \text{EF} \times \text{ED} \times 10^{-3}}{\text{BW} \times \text{AT}} \quad (2)$$

where $\text{ADD}_{\text{ingestion}}$ and $\text{ADD}_{\text{dermal}}$ represents the average daily doses from ingestion and dermal absorption of water, given as $\mu\text{g}/\text{kg}/\text{day}$, and C_w is the concentration of the trace metal in water ($\mu\text{g}/\text{l}$). IR indicates the ingestion rate of water through drinking (l/day), EF is the exposure frequency (days/year), in this study EF is 350 days/year; ED is the exposure duration (years), BW is the average body weight (kg), AT represents the average time for non-carcinogenic effects (days), SA indicates the exposed skin area (cm^2), ET is the exposure time (h/day), and K_p is the dermal permeability coefficient in water (cm/h) obtained from USEPA (2004).

Non-carcinogenic risk of trace metals was evaluated by calculating the hazard quotients (HQs). To obtain the HQs, the estimated ADDs for each trace metal are divided by the corresponding reference dose (RfD) using Eqs. 3 and 4 (Li et al. 2016, 2017, 2019).

$$\text{HQ}_{\text{ingestion/dermal}} = \frac{\text{ADD}_{\text{ingestion/dermal}}}{\text{RfD}} \quad (3)$$

$$\text{RfD}_{\text{dermal}} = \frac{\text{RfD}}{\text{ABS}_{\text{GI}}} \quad (4)$$

$$\text{HI} = \text{HQ}_{\text{ingestion}} + \text{HQ}_{\text{dermal}} \quad (5)$$

where RfD is the corresponding reference dose of the element ($\mu\text{g}/\text{kg}/\text{day}$) and ABS_{GI} is the gastrointestinal absorption factor obtained from Wang et al. (2017), Wu et al. (2009), Edokpayi et al. (2018), and USEPA (2004). The hazard index (HI) is obtained by summing the HQs of individual elements from the different pathways using Eq. 5. If

the HQ/HI is below unity or one, non-carcinogenic risk is not expected to occur; HQ/HI greater than one suggests that there may be a concern for non-carcinogenic risk or adverse effects on human health (Wang et al. 2017; Duggal et al. 2017; Barzegar et al. 2017).

Results and Discussion

Analysis of Physicochemical Parameters

The statistical results of the physicochemical parameters in groundwater samples measured during 2018 and 2019 is summarized in Table 1. The measured groundwater pH values varied from 5.3 to 8.2 and from 7.9 to 8.3 with an average value of 6.5 and 8.0 during 2018 and 2019, respectively. Approximately 75% of the samples have pH value less than 7 in 2018 indicating acidic nature of groundwater. In 2019, all the samples had pH greater than 7 suggesting alkaline

conditions (Table 1). During 2018, about 53% of the samples had pH below the World Health Organization (WHO) limit of 6.5 (WHO 2011) and all the samples were within the WHO limit in 2019. The Department of Water Affairs and Forestry of South Africa (DWAF 1996) prescribed a limit of 6.0 to 9.0 for pH (Table 1), 26% of the samples were below 6.0 during 2018 and all the groundwater samples were within this limit during 2019.

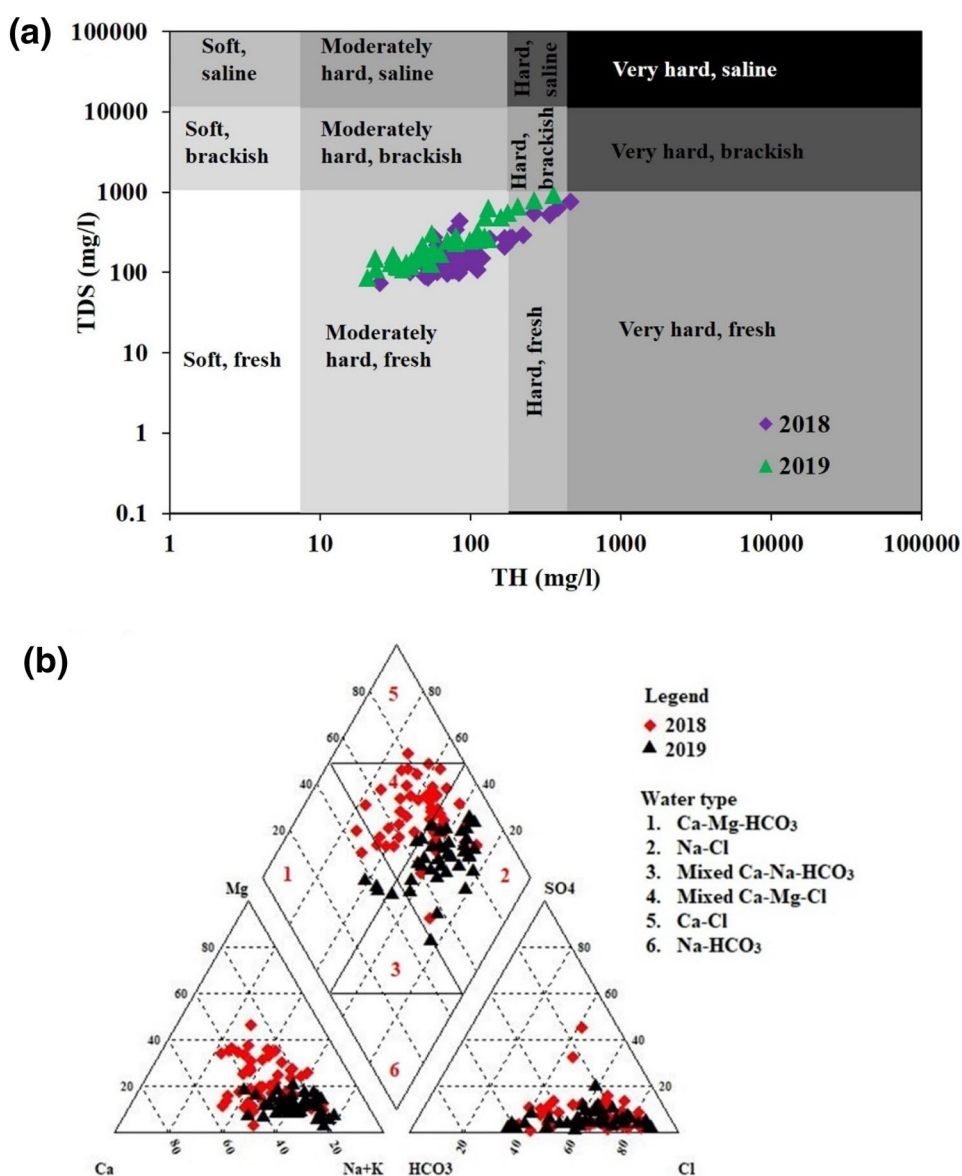
EC ranged from 115 to 1450 $\mu\text{S}/\text{cm}$ and groundwater samples were found to be within the WHO limit. However, 8% and 17% of the samples exceeded the limit established by DWAF during 2018 and 2019 respectively. Total dissolved solids (TDS) computed from the EC ranged from 74 to 764 mg/l with an average of 200 mg/l during 2018 and from 87 to 928 mg/l with an average of 258 mg/l during 2019. Total hardness (TH) calculated from calcium and magnesium varied from 25 to 464 mg/l with a mean value of 107 mg/l during 2018 and from 20 to 355 mg/l with a mean value of 79 mg/l during 2019. Bivariate plot of TDS

Table 1 Statistical parameters of analysed groundwater samples in comparison with WHO and DWAF standards

Parameters	2018 (N=53)		2019 (N=42)		Permissible limits	
	Range	Average	Range	Average	WHO (2011)	DWAF (1996)
pH	5.28–8.23	6.50	7.9–8.3	8.0	6.5–8.5	6.0–9.0
EC ($\mu\text{S}/\text{cm}$)	115–1194	312	136–1450	402.3	1500	< 700
Ca (mg/l)	4–154	27	5–97	21.9	200	< 32
Mg (mg/l)	1.2–56	9.8	1.8–28	6.0	50	< 30
Na (mg/l)	14–126	38	20–167	52.2	200	< 100
K (mg/l)	0.5–15.1	2.8	1.3–18	4.5	12.0	< 50
HCO ₃ (mg/l)	18–312	70	10–258	71.2	Not specified	Not specified
Cl (mg/l)	27–289	82.64	30–297	79.8	250	< 100
SO ₄ (mg/l)	1.8–65	13.4	2.5–38	10.3	250	< 200
F (mg/l)	BDL–1.1	0.2	–	–	1.5	< 1.0
NO ₃ (mg/l)	BDL–18	2	2–112	14.1	45	< 6
NH ₄ (mg/l)	BDL–0.2	0.0	–	–	Not specified	< 1.0
PO ₄ (mg/l)	BDL–0.5	0.1	–	–	Not specified	Not specified
As ($\mu\text{g}/\text{l}$)	BDL–3.6	0.5	–	–	10.0	< 10.0
Ag ($\mu\text{g}/\text{l}$)	–	–	BDL–13.4	3.4	Not specified	Not specified
Fe ($\mu\text{g}/\text{l}$)	2.7–770.8	88.9	23.1–20 843.2	1 521.9	300	< 100
Mn ($\mu\text{g}/\text{l}$)	0.4–84.3	19.8	1–1001.4	76	400	< 50
Al ($\mu\text{g}/\text{l}$)	1.6–3052.5	90.0	0–71.1	3.2	900	< 150
B ($\mu\text{g}/\text{l}$)	–	–	BDL–245.5	53.9	2400	–
Zn ($\mu\text{g}/\text{l}$)	1.9–19 964.5	501.4	2.5–4253.5	134.1	5000	< 3000
Pb ($\mu\text{g}/\text{l}$)	0.2–22.1	1.8	0–36.5	20	10	< 10.0
Ni ($\mu\text{g}/\text{l}$)	–	–	BDL–9.3	1.7	70	Not specified
Cr ($\mu\text{g}/\text{l}$)	–	–	BDL–8.4	4.3	50	< 50
Cu ($\mu\text{g}/\text{l}$)	BDL–279.5	19.2	0–199.6	20	2000	< 1000
Cd ($\mu\text{g}/\text{l}$)	BDL–0.2	0.0	0–4.6	3.5	3	< 5
Co ($\mu\text{g}/\text{l}$)	BDL–4.5	0.4	0–9	6	Not specified	Not specified
Li ($\mu\text{g}/\text{l}$)	300–6400	1.2	–	–	Not specified	Not specified
Sr ($\mu\text{g}/\text{l}$)	–	–	6.6–387.8	70.3	Not specified	Not specified

BDL below detection limit

Fig. 2 a Classification of groundwater based on TDS and TH, **b** hydrochemical facies of groundwater samples



versus TH (Fig. 2a) (Vetrimurugan et al. 2017a; Brindha et al. 2017) showed that majority of the samples are freshwater type (i.e. TDS < 1000 mg/l) (Freeze and Cherry 1979) with hardness ranging from moderate to very hard (Sawyer and McCarty 1978). Groundwater based on TDS indicates that the samples are moving from fresh to brackish conditions (Fig. 2a).

Evaluation of Hydrochemical Facies

Hydrochemical facies are crucial in understanding the chemical reactions which take place within the aquifer. The Piper trilinear diagram (Piper 1944) depicts that Na-Cl is the dominant groundwater type (Fig. 2b). This is common in the coastal areas due to seawater intrusion. The physical

area with Na-Cl water type had increased from 64% in 2018 to 95% in 2019 (Fig. 3a, b). Ca-HCO₃ groundwater type was also noticed. This usually indicates freshly recharging water.

Major Ion Chemistry

Based on the mean concentration of the ions measured in groundwater, the dominant order of cations and anions was Na > Ca > Mg > K and Cl > HCO₃ > SO₄ during 2018 and 2019. Sodium did not exceed the recommended limit by WHO (2011). About 8% (2018) and 14% (2019) of the samples exceeded the target water quality range established by DWAF (1996). Except for one location, potassium did not exceed the WHO limit in the study area during both sampling periods (Table 1). Calcium concentration was above

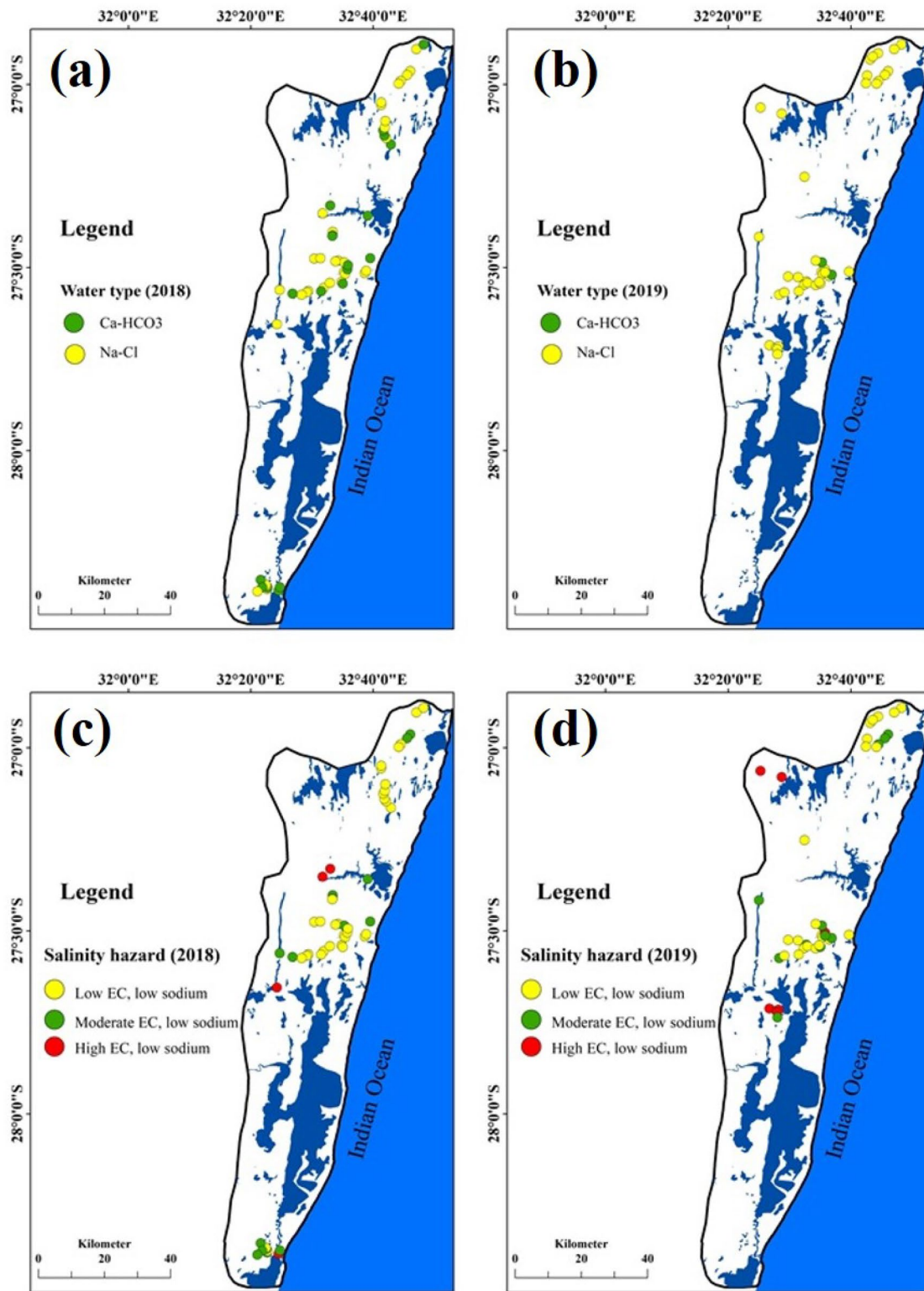


Fig. 3 Spatial distribution map showing the hydrochemical facies of groundwater samples in **a** 2018, **b** 2019 and the sodium and salinity hazard of groundwater for irrigation use in **c** 2018 and **d** 2019

the DWAf limit in 10% and 24% of the samples during 2018 and 2019, respectively. All the samples were found to be within the standard limit set by WHO and DWAf for magnesium during 2018 and 2019 except for one location which exceeded the limit during 2018. A concentration of bicarbonate below 200 mg/l is regarded as safe for human health (Bhardwaj and Singh 2011). Approximately 6% (2018) and 7% (2019) of the samples were found to have exceeded the limit. About 15% (2018) and 19% (2019) of the samples had chloride concentrations exceeding the limit recommended by DWAf while 2% of the samples were above the limit established by WHO during 2018 and 2019, respectively. Sulphate is within WHO and DWAf limits throughout the study period.

As groundwater in the study area is used for irrigation purposes, sodium adsorption ratio was plotted against the EC and this information was used to group the irrigation water types. All the groundwater samples had low sodium hazard. Figure 3c and d reveal that 55% and 66% of the groundwater samples fall in the C1S1 category during 2018 and 2019, respectively, thus implying they are suitable for irrigation. About 29% and 26% of the samples fall in the

C2S1 category during 2018 and 2019, which indicates medium salinity and low sodium hazard. The remaining 16% and 8% of the samples fall in the C3S1 category, i.e. these samples possess high salinity and low sodium hazard and may only be suitable for salt-tolerant crops. Inverse distance weighted interpolation (IDW) method was used to prepare spatial distribution maps of few major ions (Fig. 4a–h). Significant positive correlation between the spatial variation in sodium and chloride concentration in groundwater is seen in Fig. 4a and e & b and f. Similarly, calcium and bicarbonate concentrations were also high in the same areas (Fig. 4c and g & d and h). In general, calcium and bicarbonate is predominating in freshwater while seawater is dominated by sodium and chloride. Silicate weathering and dissolution of carbonate minerals increase the concentration of bicarbonate in groundwater (Elango et al. 2003; Umarani et al. 2019). High bicarbonate concentration in this study may be owed to the weathering of silicate rich sands of the KwaMbonambi and Kosi bay formations observed in the study area (Demlie et al. 2014). The high values of these four major ions in similar locations suggest that they may be due to seawater intrusion and weathering processes. Western and

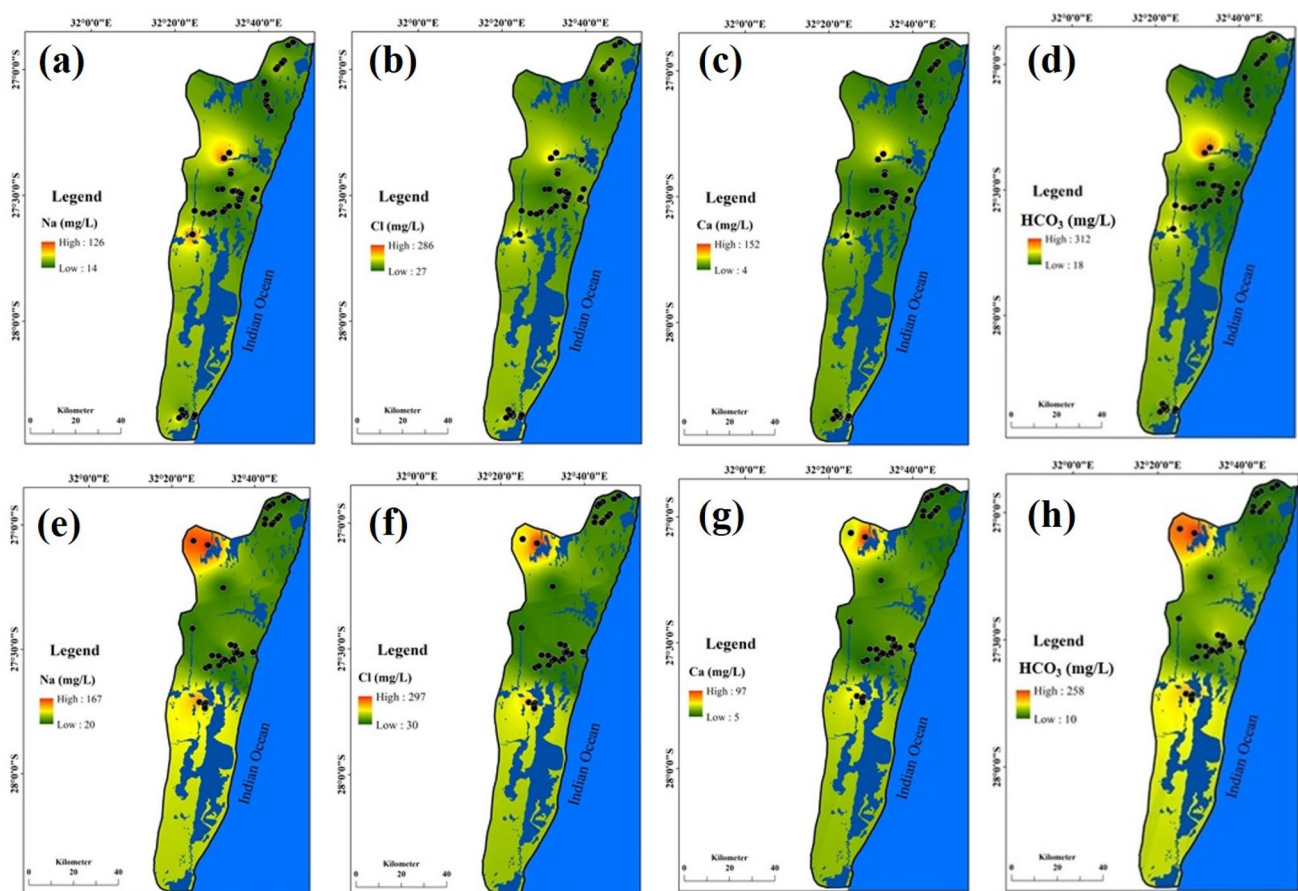


Fig. 4 Spatial distribution maps for concentrations of major ions in groundwater during 2018 (a–d) and 2019 (e–h)

southern parts of the area usually had higher concentration of all the ions. Temporally, the salinity had increased during 2018 and 2019.

Geochemical Processes

Groundwater chemistry data were used to identify the geochemical processes and mechanisms in the aquifer.

Rock Weathering

Weathering and dissolution processes were identified through various bivariate plots. Figure 5a and b indicates that groundwater chemistry is largely controlled by silicate weathering and evaporation dissolution. The scatter plot of Ca + Mg vs total cations (TC) (Fig. 5c) shows that all the samples are plotted below the 1:1 equiline with a strong positive correlation of 0.89 and 0.91 during 2018 and 2019

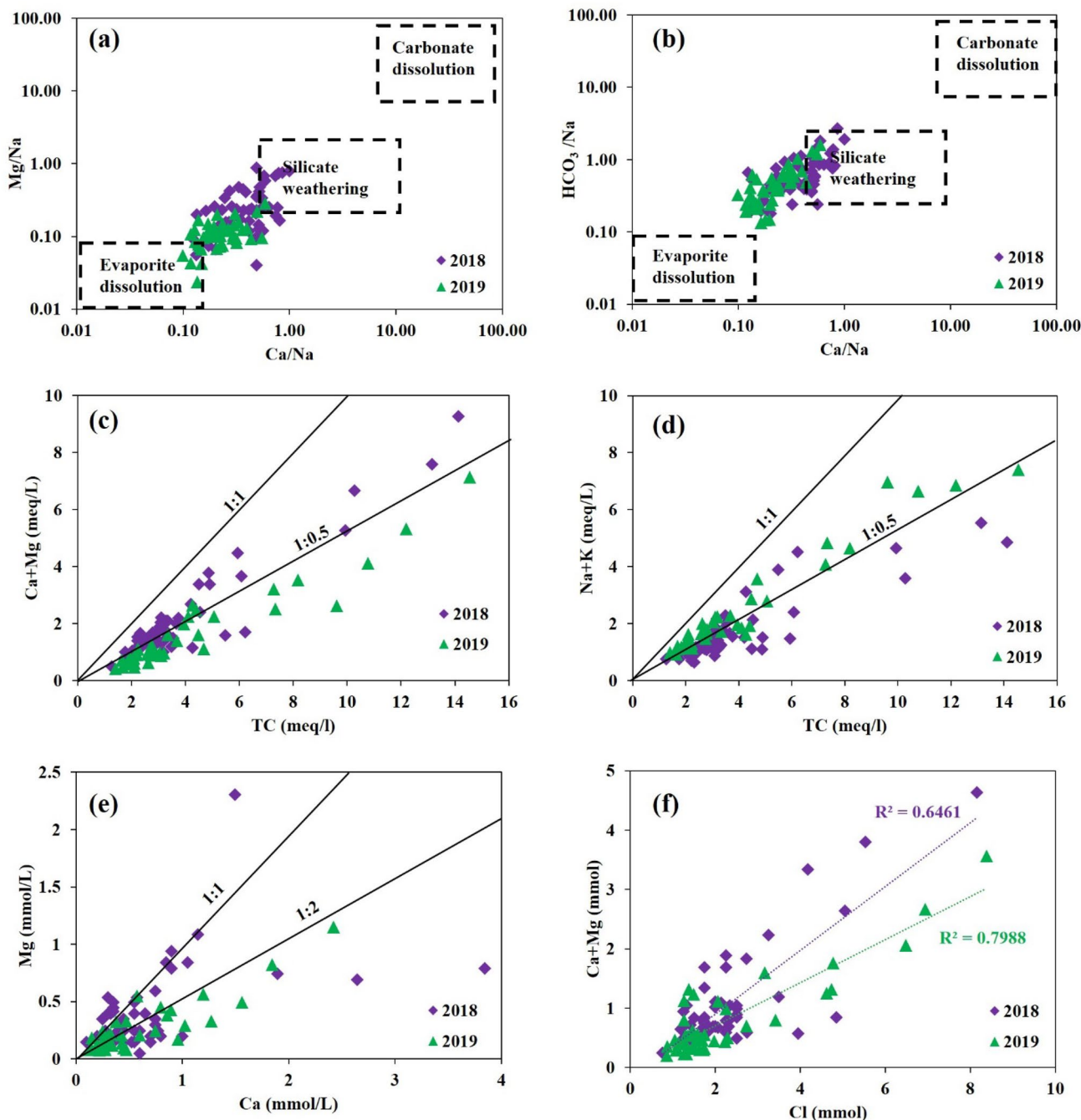


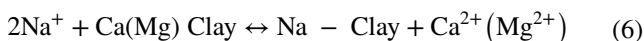
Fig. 5 Plot of a Mg/Na vs Ca/Na, b HCO₃/Na vs Ca/Na, c Ca+Mg vs TC, d Na+K vs TC, e Mg vs Ca and f Ca+Mg vs Cl

suggesting that these ions in groundwater are due to the silicate weathering process. Plot of Na + K vs TC (Fig. 5d) shows that most samples fall below and/or closer to 1:0.5 equiline with linear trend of 0.76 and 0.94 during 2018 and 2019, respectively. This infers that silicate weathering contributes to the occurrence of Na and K ions in groundwater of this area (Stallard and Edmond 1983; Vhonani et al. 2018).

Ion Exchange

The molar ratio of Ca/Mg is useful in explaining the dissolution of dolomite and calcite. Ca/Mg molar ratio equal to 1 is indicative of dissolution of dolomite (Barzegar et al. 2018a). Molar ratio between 1 and 2 reflects calcite dissolution whereas a molar ratio above 2 suggests dissolution of silicate minerals (Paul et al. 2019). In this study, the molar ratio of Ca/Mg varied from 0.6 to 12.1 during 2018 and from 0.8 to 5.7 during 2019. Few samples had a molar ratio equal to 1 implying dolomite dissolution. About 42% and 40% of the samples were between 1 and 2 during 2018 and 2019 indicating calcite dissolution. In total, 95% of the samples were greater than 2 suggesting dissolution of silicate minerals. Figure 5e also shows that most of the samples are plotted between 1:1 and 1:2 line indicating the dissolution of silicate minerals and dissolution of calcite.

Rajmohan and Elango (2004) conveyed that salinity increases with an increase in Ca + Mg and with a decline in Na/Cl ratio as a result of the reverse ion exchange process in the clay or weathered layer. The relationship between Ca + Mg vs Cl (Fig. 5f) shows that Ca + Mg increases with an increase in salinity (Zaidi et al. 2015) which is attributed to the reverse ion exchange process that is explained by the following reaction:



In a plot of sodium vs chloride, the source of sodium and chloride is explained by halite dissolution if sample points fall along the 1:1 equiline (Iqbal et al. 2018; Zaidi et al. 2015). A Na/Cl ratio above one is indicative of the silicate weathering process (Mayback 1987). In this study, the sodium vs chloride scatter plot revealed that majority of the samples fall above the 1:1 equiline (Fig. 6a). The excess chloride in groundwater is owed to the cation exchange process. The relationship between sodium vs calcium showed an enrichment of sodium over calcium (Fig. 6b) explaining the ion exchange processes (Karroum et al. 2017). Reduction of sodium with respect to chloride and depletion of calcium with respect to sodium suggests that cation exchange process controls the groundwater chemistry (Abdoul Aziz et al. 2017). The scatter diagram of Na/Cl vs Cl in Fig. 6c shows that in majority of the groundwater samples, the Na/Cl ratio

increases with a decrease in chloride concentration and vice versa. This implies that the sodium and chloride concentrations in groundwater of this area are governed by cation exchange processes (Vetrimurugan et al. 2019). Ca/SO₄ ratio closer to the 1:1 line suggests that gypsum dissolution is the source of calcium and sulphate in groundwater (Kuldip et al. 2011). Figure 6d shows a scatter plot of calcium vs sulphate which revealed that majority of the samples fall below the 1:1 equiline. This excess of calcium over sulphate in groundwater suggests that calcium is derived from dissolution of gypsum.

The plot of Ca + Mg vs HCO₃ + SO₄ (Fig. 6e) is used to determine the ion exchange process. The 1:1 equiline indicates the dissolution of gypsum, calcite and dolomite (Paul et al. 2019). If sample points are plotted below the 1:1 line (excess HCO₃ + SO₄), it means that ion exchange is the dominant process controlling groundwater chemistry, and samples falling towards Ca + Mg are indicative of the reverse ion exchange. It is depicted that majority of the samples are plotted along and above the 1:1 line indicating that the enrichment of Ca + Mg is owed to the reverse ion exchange process (Fig. 6e). The 1:2 ratios between calcium and bicarbonate suggest that calcium and bicarbonate are derived from calcite weathering whereas a 1:4 ratios are indicative of dolomite weathering. The scatter plot of calcium vs bicarbonate revealed that majority of the samples fall below and closer to the 1:2 line during 2018 and 2019 suggesting contribution of calcite weathering on groundwater chemistry (Fig. 6f).

Schoeller (1965) proposed chloro-alkaline indices (CAI 1 and CAI 2) to identify base ion exchange processes governing groundwater chemistry. The CAIs were computed by equations:

$$\text{CAI1} = \left[\frac{\text{Cl} - (\text{Na} + \text{K})}{\text{Cl}} \right] \quad (7)$$

$$\text{CAI2} = \frac{[\text{Cl} - (\text{Na} + \text{K})]}{[\text{Cl} + \text{HCO}_3 + \text{SO}_4 + \text{NO}_3]} \quad (8)$$

A positive CAI is indicative of reverse ion exchange between sodium and potassium in groundwater with calcium and magnesium in the aquifer material. Ion exchange is shown by negative index which suggests an exchange of sodium and potassium in the aquifer matrix and calcium and magnesium in groundwater. CAIs can also be used to determine the origin of bicarbonate in groundwater. Positive values of CAIs suggest the weathering and dissolution of silicate minerals and negative values represent dissolution of carbonate minerals. In this study, approximately 94% (2018) and 48% (2019) of the samples were positive for both CAI 1 and CAI 2. Figure 7a shows that reverse ion exchange is the major process governing groundwater

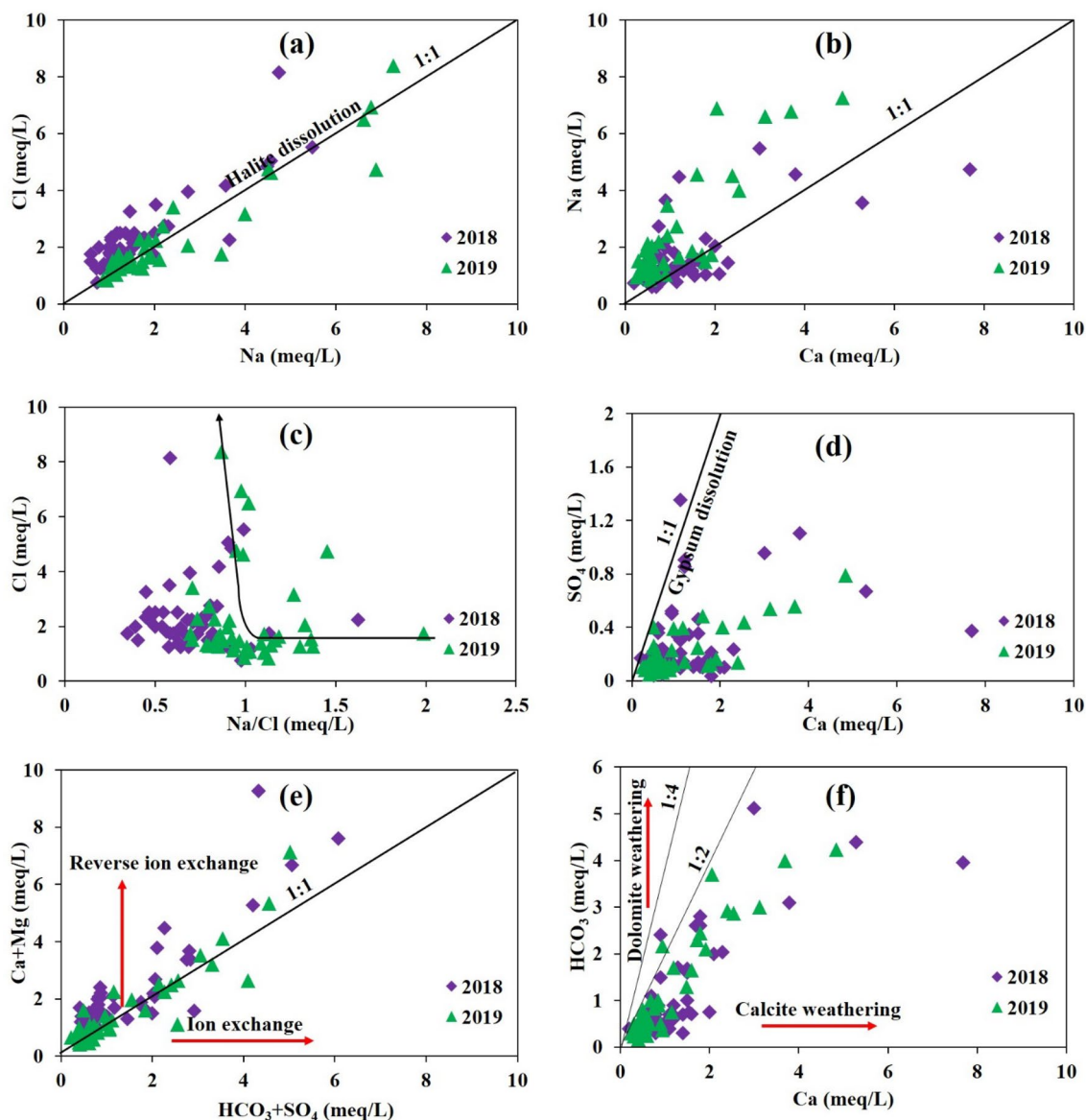


Fig. 6 Plot of **a** Na vs Cl, **b** Ca vs Na, **c** Na/Cl vs Cl, **d** Ca vs SO_4 , **e** $\text{HCO}_3 + \text{SO}_4$ vs Ca + Mg and **f** Ca vs HCO_3

chemistry during 2018 while ion exchange is dominant during 2019. Bicarbonate in groundwater results from the weathering and dissolution of silicate minerals during 2018 and by dissolution of carbonate minerals in 2019.

Chadha diagram (Chadha 1999) was used to comprehend the geochemical processes that influence the chemistry of groundwater. It is expressed as the difference between alkaline earths (Ca + Mg) and alkali metals (Na + K) and difference between weak acids ($\text{CO}_3 + \text{HCO}_3$) and strong acids (Cl + SO_4) in milliequivalent percentage. Figure 7b, it is depicted that majority of the samples fall in the field of reverse ion exchange and the seawater type during 2018 and 2019, respectively. This further support

that reverse ion exchange and seawater intrusion are the dominant processes in the study area.

Impact of Seawater Intrusion

The Na/Cl molar ratio vs Cl is commonly used to evaluate the influence of seawater into groundwater (Abu-alnaeem et al. 2018; Seddique et al. 2019; Telahigue et al. 2018; Tiwari et al. 2019). Values closer to the seawater ratio (0.86) suggest that groundwater is contaminated by seawater. In this study, the Na/Cl ratio varied from 0.3 to 1.6 with an average of 0.7 during 2018 and from 0.7 to 2 with an average value of 1 during 2019. Approximately 6% (2018) and

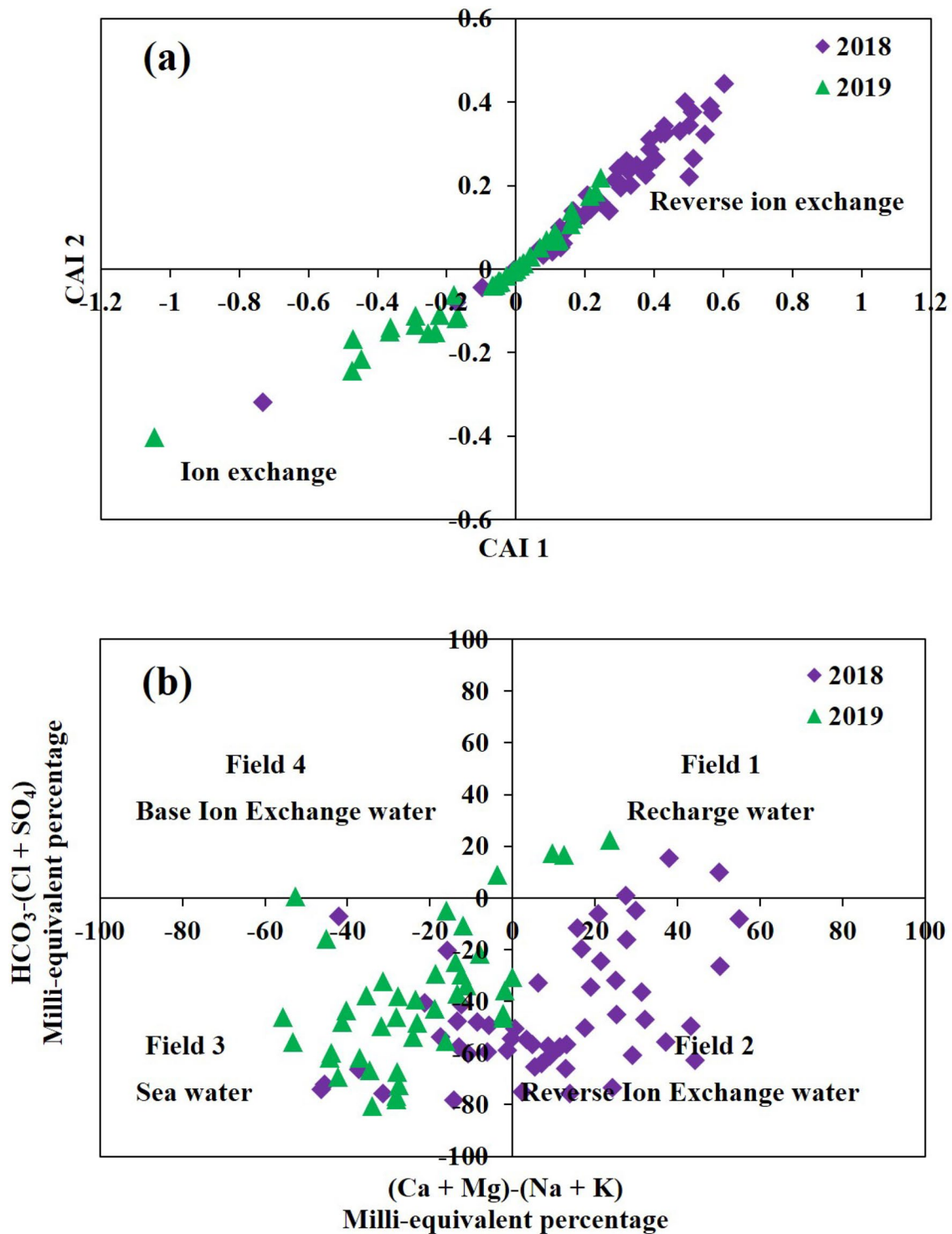


Fig. 7 a CAIs indicating base ion exchange processes in groundwater, **b** Chadha diagram showing hydrogeochemical processes in groundwater

10% (2019) of the samples fall closer to the seawater ratio due to saline water mixing (Fig. 8a). The remaining samples are plotted below and above the seawater ratio suggesting that groundwater is influenced by saline water and anthropogenic activities. The Cl/HCO_3 ratio is widely used

to examine groundwater salinization due to mixing with seawater (Yohana et al. 2013; Kanagaraj et al. 2018). The Cl/HCO_3 ratio can be classified into three categories; unaffected (<0.5), slightly or moderately affected ($0.6\text{--}6.6$), and strongly affected (>6.6) by salinization process (Revelle

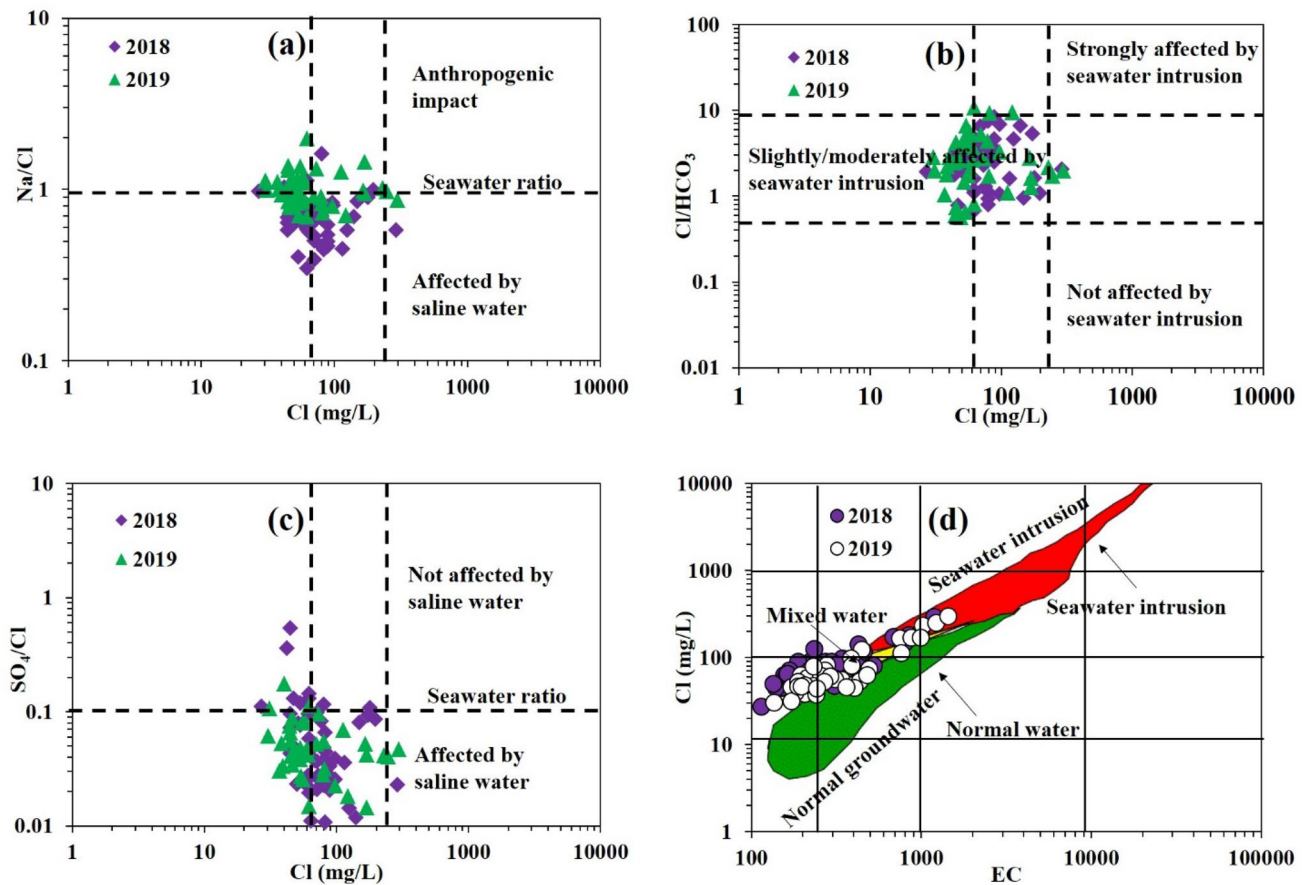


Fig. 8 Plots explaining the seawater intrusion **a** Na/Cl vs Cl, **b** Cl/HCO₃ vs Cl, **c** SO₄/Cl vs Cl and **d** Cl vs EC

1941). In this study, the Cl/HCO₃ ratio varied from 0.7 to 8.3 with an average of 3.02 during 2018 and from 0.6 to 10.7 with an average value of 3.1 (Fig. 8b).

A plot of SO₄/Cl vs Cl with values above 0.1 implies that groundwater is not affected by seawater and samples with values below 0.1 are affected by seawater intrusion (Kanagaraj et al. 2018). About 23% (2018) and 10% (2019) of the samples had SO₄/Cl values greater than 0.1 suggesting that they are not contaminated by seawater while 77% (2018) and 90% (2019) of the samples were below 0.1 indicating the influence of seawater intrusion (Fig. 8c). Most of the groundwater samples were slightly or moderately affected by seawater intrusion. The scatter diagram of EC vs chloride indicates that majority of the samples fall in the mixed and few in the seawater zone during 2018 and 2019 (Fig. 8d).

Seawater Mixing Index

The seawater mixing index (SMI) which was established by Park et al. (2005) is widely employed to identify seawater mixing based on four major ions such as Na, Mg, Cl and

SO₄ (Vetrimurugan et al. 2017a; Seddique et al. 2019). It is computed using the following equation:

$$SMI = a \times \frac{C_{Na}}{T_{Na}} + b \times \frac{C_{Mg}}{T_{Mg}} + c \times \frac{C_{Cl}}{T_{Cl}} + d \times \frac{C_{SO_4}}{T_{SO_4}} \quad (9)$$

where the constants a , b , c and d represent the relative concentration proportions of the four major ions in seawater with Na ($a=0.31$), Mg ($b=0.04$), Cl ($c=0.57$) and SO₄ ($d=0.08$). C is the measured concentration of ions in mg/l and T is the regional threshold value. Cumulative probability curves plotted against log concentration of ions is used to estimate the regional threshold values of the ions. Regional threshold values estimated in this study are indicated by inflection points in Fig. 9a–d. Regional threshold values such as Na = 53 mg/l, Mg = 20 mg/l, Cl = 97 mg/l and two inflection points were identified as 3 and 19 mg/l for SO₄ during 2018 and Na = 80 mg/l, Mg = 14 mg/l, Cl = 121 mg/l and SO₄ was 4 and 23 mg/l during 2019. In this study, the highest value of the inflection point was chosen for SO₄, i.e. 19 and 23 mg/l for 2018 and 2019. A SMI value greater than one suggests the impact of seawater mixing with fresh

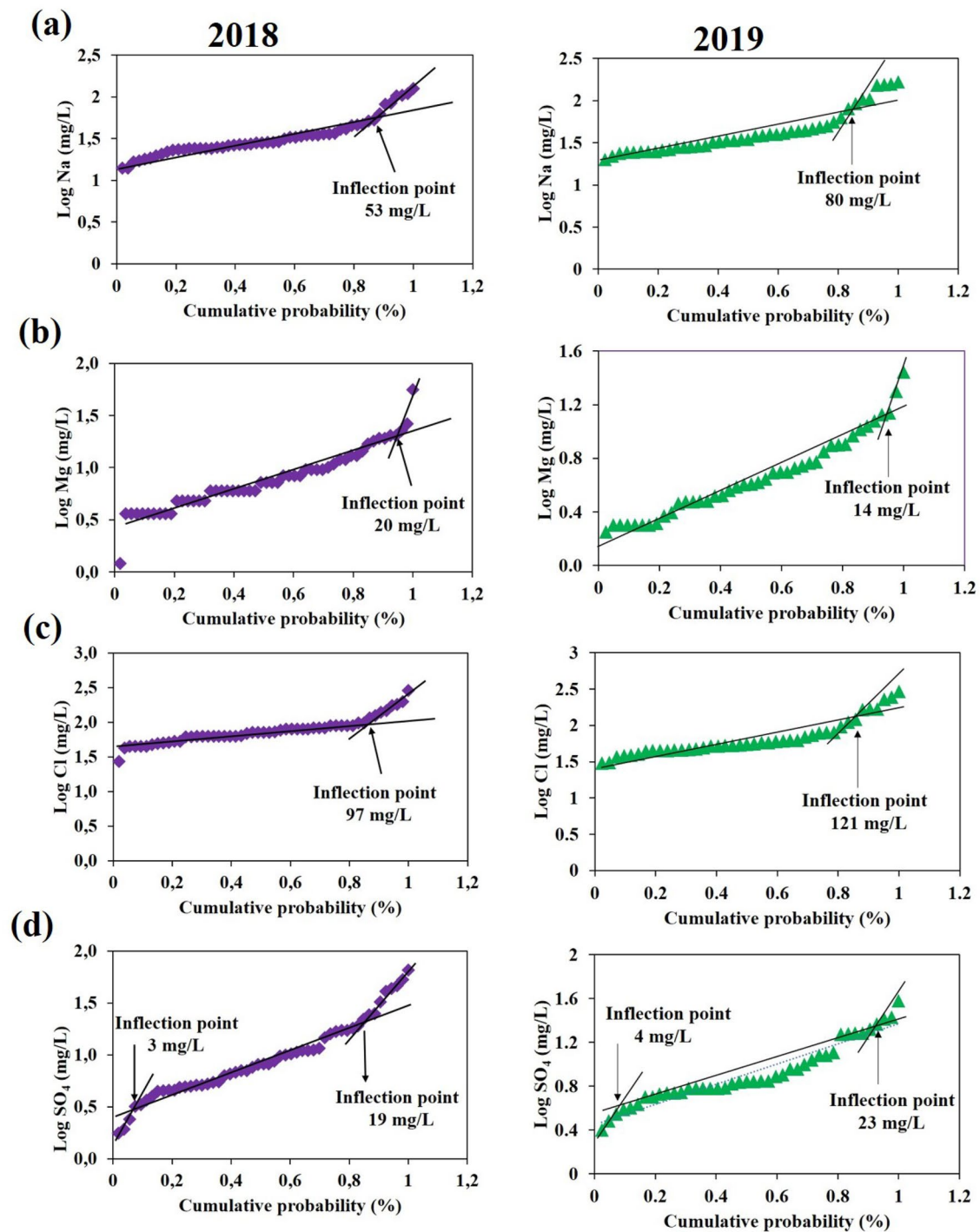


Fig. 9 a–d Cumulative probability distribution during 2018 and 2019

water. In this study, the SMI varied from 0.3 to 2.5 during 2018 and from 0.3 to 2.3 during 2019. About 15% and 14% of groundwater has a SMI above one during 2018 and 2019, respectively. This suggests that groundwater chemistry is influenced by mixing with saline water.

Nutrients

Nitrate occurs naturally at very low concentrations in groundwater and is regarded as an important plant nutrient. Common sources of nitrate in groundwater are from

inorganic fertilizers and manures, wastewater disposal on land for irrigation and oxidation of nitrogenous waste products in human or animal excreta (Vetrimurugan et al. 2017c; He et al. 2020). In this study, nitrate ranged up to 112 mg/l with an average of 2 and 14 mg/l during 2018 and 2019 (Table 1), respectively. The nitrate concentration in groundwater has increased in 2019 at two locations which is due to anthropogenic sources like application of agricultural fertilizers. This led to nitrate concentrations exceeding the WHO limit in 5% of the locations. Nitrate contamination is usually associated with shallow groundwater (He et al. 2020). Still and Nash (2002) reported that pit latrines and public water points are observed to influence nitrate concentrations in groundwater of Maputaland. This may also be another reason for an increase in nitrate concentration in groundwater of the study area.

Natural levels of ammonia in groundwater are usually below 0.2 mg/l (WHO 1996). However, elevated concentrations are indicative of bacterial, sewage and animal waste pollution. In this study, ammonia ranged from 0 to 0.2 mg/l. Phosphate is another essential element for plant life. In the study area, it ranged up to 0.5 mg/l with an average of 0.1 mg/l. Both ammonia and phosphate were in low concentrations and were not a threat to groundwater quality (Table 1). Sources of phosphate include decomposition of rocks and minerals, agricultural runoff, sewage, industrial runoff, aquaculture activities, etc. (Vetrimurugan et al. 2013, 2017c; Sharma and Bhattacharya 2017).

Trace Metals in Groundwater

The concentrations of analysed trace metals is summarized in Table 1. A total of ten and thirteen trace metals were analysed during 2018 and 2019, respectively. Trace metals such as As, Ag, B, Ni, Cr, Cu, Cd and Co recorded minimum values below the detection limits in some sampling locations. The mean concentrations of the trace metals in groundwater were found in the following order during 2018: Zn > Li > Al > Fe > Mn > Cu > Pb > As > Co > Cd and the following descending order during 2019: Fe > Zn > Mn > Sr > B > Pb > Cu > Co > Cr > Cd > Ag > Al > Ni. Iron in groundwater of this area was found to have exceeded the DWAF limit in 19% and 48% of the samples during 2018 and 2019, respectively. Likewise, 9% and 24% of the samples were found to have exceeded the WHO limit during 2018 and 2019, high iron content resulting from the leaching of iron-rich sediments (Ahmed et al. 2019). Concentrations of manganese were found to be above the standard limit proposed by DWAF in 13% and 26% of the samples during 2018 and 2019. Likewise, manganese concentration exceeded the WHO standard limit in 7% of the samples during 2019. About 6% and 2% of the samples had aluminium concentrations above the limit established by DWAF and WHO for drinking water during

2018 while all the samples were within the limit during 2019. The concentration of zinc in groundwater was found to have exceeded the DWAF and WHO standard limit in 4% and 2% of the samples during 2018. Approximately 2% of the samples had zinc in groundwater above the DWAF limit during 2019. Lead in groundwater of this area was above the limit of DWAF and WHO in 2% and 86% of the samples during 2018 and 2019, respectively. The concentration of cadmium in groundwater of this area was found to be within the DWAF/WHO limits during 2018. However, 86% of the samples had cadmium concentration above the limit of 3 µg/l proposed by WHO during 2019. Contents of copper, arsenic, boron, chromium and nickel were found to be below the established WHO and DWAF standard values. The Mbazwana landfill lying within the study area is used for the disposal of domestic wastes and garden refuse. Landfill, agricultural activities and seawater intrusion might be the source of high concentrations of iron, manganese, zinc and lead in groundwater of this area (Asma et al. 2013; Vetrimurugan et al. 2017b; Ahmed et al. 2019).

Anthropogenic Activities

Subsistence farming and commercial forestry plantations are widely practised in the study area. The plot of HCO_3 vs TC is used to evaluate the influence of anthropogenic activities on groundwater quality. Samples plotting on the 1:1 line are indicative of the dominance of dissolution of silicates and carbonates. Sample points plotted below the 1:1 line suggest the influence of anthropogenic activities. Figure 10a reveals that all the samples are plotted below the 1:1 line. This indicates the influence of anthropogenic activities like waste disposal and agricultural activities. The plot of TDS vs $\text{NO}_3 + \text{Cl} + \text{SO}_4/\text{HCO}_3$ was also employed to further evaluate the contribution of anthropogenic activities (especially from agricultural activities) on groundwater chemistry. A high correlation between $\text{NO}_3 + \text{Cl} + \text{SO}_4/\text{HCO}_3$ and TDS is attributed to the use of agricultural fertilizers (Barzegar et al. 2018a). Figure 10b shows a strong correlation of $R^2 = 0.96$ (2018) and $R^2 = 0.99$ (2019). It further reveals that groundwater chemistry in the study area is impacted by agricultural activities which mainly results from excessive application of fertilizers. This could also be the source for the presence of trace metals in groundwater due to use of agrochemicals in the farming land.

Correlation Matrix

Correlation matrix was used to evaluate the interrelationship between parameters. Values > 0.7 indicate strong positive correlation, values between 0.5 and 0.7 indicate moderate correlation and values between 0.5 and 0.3 indicate weak correlation. Correlation matrix of measured variables is

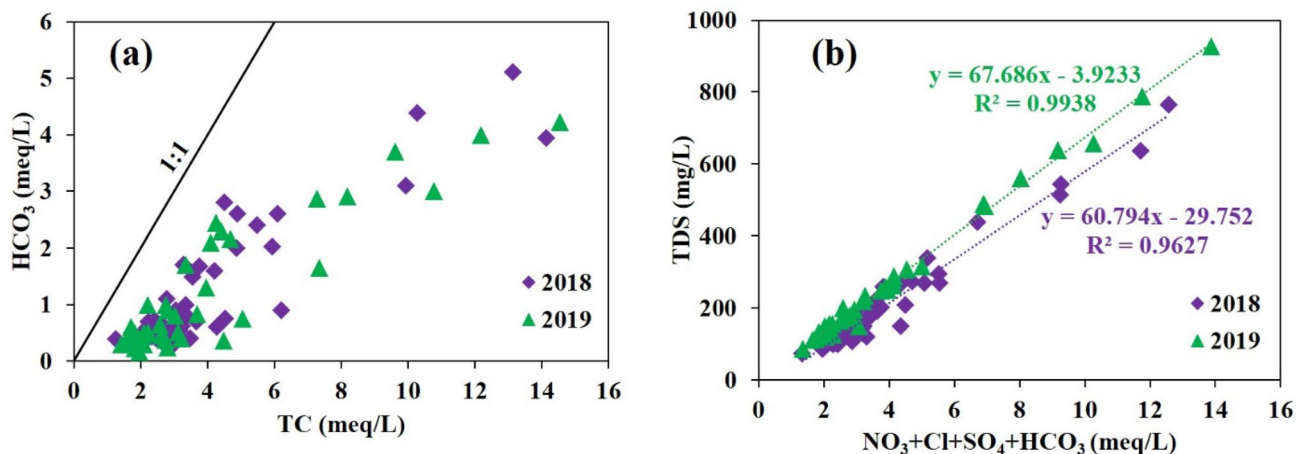


Fig. 10 Plot of **a** HCO₃ vs TC and **b** TDS vs NO₃+Cl+SO₄/HCO₃

outlined in Table 2. Strong and moderate correlations persist between EC and most major ions. The strong positive correlation of EC with the other major ions suggests that the major processes controlling the groundwater chemistry of this area are ion exchange and seawater intrusion. Hence, these ions contribute to groundwater salinity. The strong correlation between sodium and chloride is indicative of a common source of origin which is from excessive evaporation process, dissolution of halite rock and anthropogenic activities. Calcium strongly correlates with chloride and bicarbonate during 2018 and showed strong correlation with magnesium ($r=0.9$), chloride ($r=0.9$), bicarbonate ($r=0.9$) and sulphate ($r=0.8$) during 2019. Strong correlation between calcium and bicarbonate indicates that calcite dissolution could be the possible sources of calcium in groundwater of this area (Barzegar et al. 2017). The good correlation between calcium and magnesium is owed to the dissolution of calcium–magnesium-bearing minerals such as calcite, aragonite, dolomite and clays (Papazotos et al. 2019). The strong correlation between calcium and sulphate suggests contribution from sulphate minerals such as gypsum (Soltani et al. 2017; Esmaili et al. 2018) and correlation between calcium and chloride is indicative of the reverse ion exchange process. Chloride shows strong positive correlation with bicarbonate ($r=0.81$) during 2018 and a strong correlation with bicarbonate ($r=0.78$) and sulphate ($r=0.79$) during 2019. The high chloride concentration when compared to sulphate suggests sulphate reduction (Elango et al. 2003; Vhonani et al. 2018) (Table 2).

Health Risk Assessment

Health risk assessment was used to evaluate the health risk that trace metals may pose on humans through oral ingestion and dermal absorption. Tables 3 and 4 show the values

of parameters used for health risk assessment in this study. Health-related risk associated with exposure to trace metals was determined using the concentration of a total of eleven trace metals including As, Cu, Pb, Co, Cd, Mn, Fe, Al and Zn during 2018 and Cu, Pb, Co, Cd, Mn, Fe, Zn, Cr and Ni for 2019, respectively. The average HQs and HI values of the trace metals via ingestion and dermal absorption pathways are presented in Table 5, respectively. The calculated mean values of HQ_{ingestion} and HQ_{dermal} in the study area decreased in the order of Zn > As > Co > Pb > Mn > Cu > Fe > Al > Cd and Mn > Zn > Co > Cu > As > Cd > Fe > Al > Pb, for both adults and children during 2018, respectively. The HQ_{ingestion} and HQ_{dermal} was in the order of Co > Pb > Cd > Mn > Fe > Cr > Zn > Cu > Ni and Cd > Mn > Cr > Co > Fe > Pb > Cu > Zn > Ni, for both adults and children during 2019. This suggests that arsenic, cobalt, lead, and zinc are major contributors to the ingestion exposure for both age groups in the study area. Regarding the dermal exposure, manganese, cadmium, and zinc were observed to have more potential non-carcinogenic concerns for both age groups. The HQ_{ingestion} values for both adults and children were less than one for all trace metals during 2018 (Fig. 11a), indicating that they pose little hazard. The mean HQ_{ingestion} values for lead and cobalt were greater than one for children during 2019 (Fig. 11b). This implies that these metals pose serious to adverse health effects on children and are major contributors to ingestion exposure. The HQ_{dermal} values for both adults and children in all trace metals were below one during 2018 and 2019, respectively. This suggests that the concentration of these metals pose a minimum hazard to people through dermal exposure pathway. For children, the total hazard index (HI) values ranged from 8.9E–2 to 8.35E+0 and from 1.2E–2 to 1.3E+1 with average values of 9.3E–1 and 6.0E+0 during 2018 and 2019, respectively. The HI average values for the study area were higher than the acceptable limit of

Table 2 Correlation matrix of groundwater quality variables during 2018 and 2019

	pH	EC	Na	K	Ca	Mg	Cl	HCO ₃	SO ₄	NO ₃
2018										
pH	1									
EC	0.32	1								
Na	0.22	0.91	1							
K	0.04	0.18	0.29	1						
Ca	0.19	0.85	0.65	0.04	1					
Mg	0.10	0.64	0.50	-0.05	0.49	1				
Cl	0.10	0.90	0.87	0.26	0.82	0.49	1			
HCO ₃	0.27	0.87	0.71	0.07	0.78	0.81	0.66	1		
SO ₄	0.22	0.53	0.57	-0.07	0.33	0.32	0.33	0.40	1	
NO ₃	0.08	0.19	0.26	0.09	0.09	-0.01	0.28	-0.04	-0.01	1
2019										
pH	1									
EC	0.10	1								
Na	0.09	0.97	1							
K	0.09	0.11	0.08	1						
Ca	0.11	0.95	0.86	0.05	1					
Mg	0.06	0.88	0.79	0.15	0.89	1				
Cl	0.11	0.95	0.94	0.18	0.87	0.87	1			
HCO ₃	0.03	0.91	0.86	-0.01	0.93	0.76	0.78	1		
SO ₄	0.09	0.83	0.83	-0.04	0.77	0.74	0.79	0.69	1	
NO ₃	0.15	0.26	0.25	-0.02	0.22	0.37	0.15	0.15	0.39	1

Bold significant correlation (p 0.05)

Table 3 Human exposure parameter values

	IR (l/day)	ED (years)	BW (kg)	AT (days)	SA (cm ²)	ET (h/day)
Adults	2.2	70	70	25,550	18,000	0.58
Children	1.8	6	15	2190	6600	1

Table 4 K_p and RfD for the analysed trace metals

Trace metal	K_p (cm/h)	RfD _{ingestion} (µg/kg/day)	RfD _{dermal} (µg/kg/day)
As ^a	1×10^{-3}	0.3	0.285
Cu ^b	1×10^{-3}	40	8
Pb ^b	1×10^{-4}	1.4	0.42
Ni ^b	2×10^{-4}	20	0.8
Co ^b	4×10^{-4}	0.3	0.06
Cr ^b	1×10^{-3}	3	0.075
Cd ^b	1×10^{-3}	0.5	0.025
Mn ^b	1×10^{-3}	24	0.96
Fe ^b	1×10^{-3}	700	140
Al ^b	1×10^{-3}	1000	200
Zn ^b	6×10^{-4}	300	60

^aWu et al. (2009)^bWang et al. (2017)^cUSEPA (2004)

one during 2019, indicating that trace metal concentrations may pose non-carcinogenic health risks for children. The HI values for adults ranged from $2.3E-2$ to $2.2E+0$ and from $3.1E-3$ to $3.3E+0$ with average values of $2.4E-1$ and $1.6E+0$, during 2018 and 2019, respectively. The HI average values exceeded the acceptable limit during 2019, implying

that the concentration of trace metals in groundwater may cause serious to adverse health effects on adults. Similarly, Fig. 11c shows that average HI of all the trace metals were below unity in both adults and children in 2018 whereas the average HI values for lead and cobalt exceeded unity in children during 2019 (Fig. 11d). Figure 12a–d shows the spatial distribution of HI values for children and adults during 2018 and 2019. The HI values for adults during 2018 and 2019 were classified into two levels of chronic risk comprising low (96% and 14% samples during 2018 and 2019) and medium (4% and 86% samples during 2018 and 2019, respectively) (Table 6). HI values for children were classified in terms of three levels including low (84% and 12% of samples), medium (14% and 2% of samples), and high (2% and 86% of samples) during 2018 and 2019, respectively. This implies that chronic risk level is high in children as compared to adults. This also concludes that children and adults face higher non-carcinogenic health risk during 2019 as compared to 2018. This is due to the rise in concentrations of trace metals found in 2019.

Conclusion

In this study, groundwater samples were collected from the Maputaland coastal plain, South Africa, and were analysed. Geostatistical and GIS methods were applied to identify the

Table 5 Non-carcinogenic health risk of trace metals by ingestion and dermal absorption pathway

Trace metal	HQ _{ingestion} (µg/kg/day)				HQ _{dermal} (µg/kg/day)				HI			
	2018		2019		2018		2019		2018		2019	
	Adult	Children	Adult	Children	Adult	Children	Adult	Children	Adult	Children	Adult	Children
As	4.98E-2	1.90E-1	–	–	2.49E-4	7.34E-4	–	–	5.00E-2	1.91E-1	–	–
Cu	1.51E-2	5.77E-2	9.82E-3	3.75E-2	3.58E-4	1.06E-3	2.33E-4	6.87E-4	1.55E-2	5.87E-2	1.01E-2	3.82E-2
Pb	3.96E-2	1.51E-1	4.48E-1	1.71E+0	6.27E-5	1.85E-4	7.09E-4	2.09E-3	3.97E-2	1.51E-1	4.49E-1	1.71E+0
Ni	–	–	2.60E-3	9.92E-3	–	–	6.17E-5	1.82E-4	–	–	2.66E-3	1.01E-2
Co	4.64E-2	1.77E-1	6.31E-1	2.41E+0	4.41E-4	1.30E-3	5.99E-3	1.77E-2	4.69E-2	1.79E-1	6.37E-1	2.43E+0
Cr	–	–	4.54E-2	1.73E-1	–	–	8.61E-3	2.54E-2	–	–	5.40E-2	1.99E-1
Cd	2.39E-3	9.11E-3	2.19E-1	8.35E-1	2.26E-4	6.68E-4	2.08E-2	6.12E-2	2.61E-3	9.77E-3	2.39E-1	8.96E-1
Mn	2.59E-2	9.90E-2	9.95E-2	3.80E-1	3.07E-3	9.07E-3	1.18E-2	3.48E-2	2.90E-2	1.08E-1	1.11E-1	4.15E-1
Fe	3.99E-3	1.52E-2	6.83E-2	2.61E-1	9.47E-5	2.79E-4	1.62E-3	4.78E-3	4.09E-3	1.55E-2	7.00E-2	2.66E-1
Al	2.83E-3	1.08E-2	–	–	6.71E-5	1.98E-4	–	–	2.90E-3	1.10E-2	–	–
Zn	5.25E-2	2.01E-1	1.41E-2	5.37E-2	7.48E-4	2.21E-3	2.00E-4	5.90E-4	5.33E-2	2.03E-1	1.43E-2	5.42E-2

Values shown in bold letters are with HQ/HI > 1

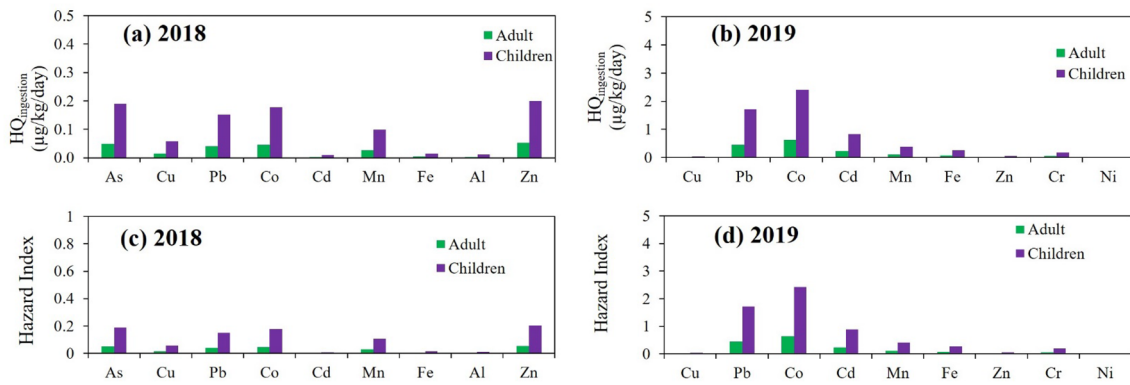


Fig. 11 Human health risk based on $HQ_{\text{ingestion}}$ (a, b) and hazard index (c, d) during 2018 and 2019

hydrogeochemical processes that control the groundwater chemistry of the study area. The potential non-carcinogenic health risk of trace metals through ingestion and dermal absorption pathways was assessed. The following conclusions are summarized:

- Groundwater was acidic to alkaline in nature. Based on TDS and TH classification, groundwater belongs to soft and hard freshwater type. In general, groundwater quality is suitable for drinking purposes except in a few locations at which some groundwater quality parameters such as Na, Cl, Ca and Mg exceeded the DWAf and WHO drinking water limits. All trace metals were within WHO standards for drinking water except Cd, Zn, Pb, Mn, Al and Fe. Na–Cl water type is the dominant groundwater type followed by Ca– HCO_3 .
 - Hydrogeochemical processes controlling groundwater chemistry were rock-water interaction, silicate weathering, reverse ion exchange, seawater intrusion and anthropogenic activities. Increased concentration of some major ions with increase in salinity owes to the reverse ion exchange process. The SMI ranges from 0.3 to 2.5 and from 0.3 to 2.3 during 2018 and 2019, respectively. Approximately, 29% of groundwater had high SMI values, suggesting contamination by seawater intrusion.
- Statistical analysis also confirmed the geochemical processes identified.
- Trace metal analysis showed that arsenic, cobalt, cadmium, lead, manganese and zinc were the main contributors to non-carcinogenic risk through oral ingestion pathway. The mean value of $HQ_{\text{ingestion}}$ and HI value for cobalt and lead had the highest contribution to the total non-carcinogenic risk in the study area. The HQ_{dermal} was less than unity implying that trace metal pose less significant health risk to adults and children through dermal absorption pathway. According to the classification of chronic risk, adults in the study area fall into two levels of risk including low and medium; children fall into three levels of risk including low, medium and high risk. This concludes that chronic risk level is high in children than compared to adults.
 - Long-term monitoring and assessment of trace metals is necessary to minimize health effects from consuming groundwater on local people. These findings have produced a baseline dataset for further systematic investigation and other involved water management sectors to consider the study findings and to utilize it in further improvement, development and protection of groundwater resources and health of the human population residing in the study area.

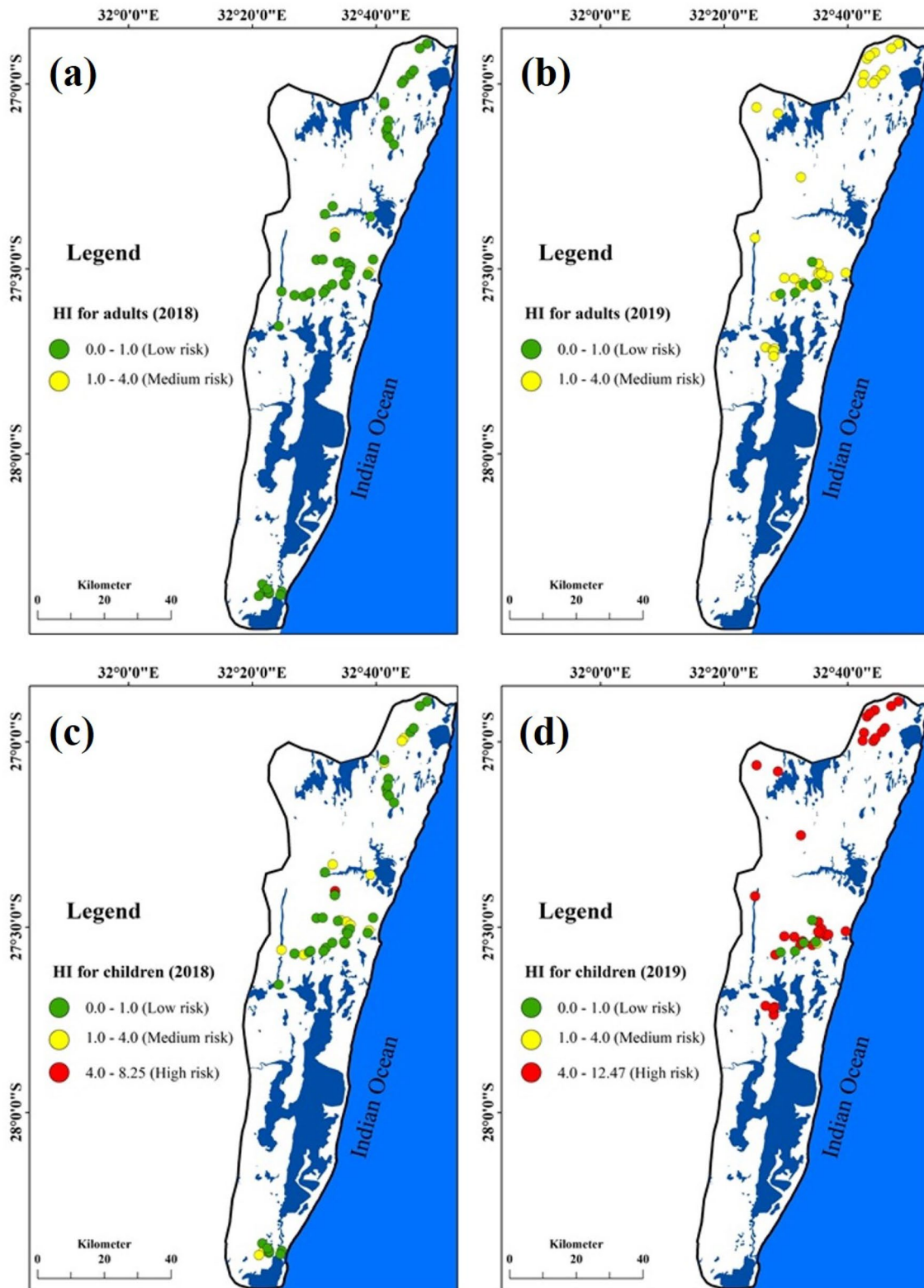


Fig. 12 Spatial variation of hazard index of trace metals in groundwater during 2018 and 2019

Table 6 Classification of chronic (non-carcinogenic) risk (USEPA 1999)

Risk level	HI	Chronic risk
1	< 0.1	Negligible
2	≥ 0.1 < 1	Low
3	≥ 1 < 4	Medium
4	≥ 4	High

Acknowledgements Authors from the University of Zululand express their gratitude to National Research Foundation (NRF), South Africa (NRF/NSFC Reference: NSFC170331225349, Grant No: 110773), for providing grants and Department of Research and Innovation, the University of Zululand for support in buying Ion Chromatography instrument for this research. iSimangaliso Wetland Park Authority is thanked for permission to collect the water samples in the Park. Dr. Peiyue Li is grateful for the financial support granted by the National Natural Science Foundation of China (41761144059).

References

- Abdoul Aziz G, Philippe O, Julie G, Fatou DN, Alain D, Raymond M, Serge B (2017) Factors controlling the evolution of groundwater dynamics and chemistry in the Senegal River Delta. *J Hydrol Reg Stud*. <https://doi.org/10.1016/j.ejrh.2017.01.005>
- Abu-alnaeem MF, Yusoff I, Ng TF, Alias Y, Raksmei M (2018) Assessment of groundwater salinity and quality in Gaza coastal aquifer, Gaza Strip, Palestine: an integrated statistical, geostatistical and hydrogeochemical approaches study. *Sci Total Environ* 615:972–989
- Ahmed N, Bodrud-Doza M, Islam ARMT, Hossain S, Moniruzzaman M, Deb N, Bhuiyan ABQ (2019) Appraising spatial variations of As, Fe, Mn and NO₃ contaminations associated health risks of drinking water from Surma basin, Bangladesh. *Chemosphere* 218:726–740
- APHA (American Public Health Association) (2012) Standard methods for the examination of water and wastewater, 22nd edn. APHA-AWWA-WEF, Washington
- Askri B, Ahmed AT, Al-Shanfari RA, Bouhlila R, Al-Farisi KBK (2016) Isotopic and geochemical identifications of groundwater salinisation processes in Salalah coastal plain, Sultanate of Oman. *Chem Erde Geochem* 76:243–255
- Asma BH, Sohail KAHM, Selim R, Mohammad NZ, Mohammad AA, Mohammad AA, Mohammad MR (2013) Trace metals pollution in seawater and groundwater in the ship breaking area of Sitakund Upazilla, Chittagong, Bangladesh. *Mar Pollut Bull* 71:317–324
- Barzegar R, Asghari A, Shahla M, Elham S, Evangelos F (2017) Heavy metal (loid) s in the groundwater of Shabestar Area (NW Iran): source identification and health risk assessment. *Expo Health* 11(4):251–265
- Barzegar R, Asghari MA, Adamowski J, Nazemi AH (2018a) Assessing the potential origins and human health risks of trace elements in groundwater: a case study in the Khoi plain, Iran. *Environ Geochem Health* 41(2):981–1002. <https://doi.org/10.1007/s10653-018-0194-9>
- Barzegar R, Asghari Moghaddam A, Nazemi AH, Adamowski J (2018b) Evidence for the occurrence of hydrogeochemical processes in the groundwater of Khoi plain, northwestern Iran, using ionic ratios and geochemical modeling. *Environ Earth Sci* 77(16):1–17. <https://doi.org/10.1007/s12665-018-7782-y>
- Bhardwaj V, Singh DS (2011) Surface and groundwater quality characterization of Deoria District, Ganga Plain, India. *Environ Earth Sci* 63(2):383–395
- Bouzourra H, Bouhlila R, Elango L, Slama F, Ouslati N (2015) Characterization of mechanisms and processes of groundwater salinization in irrigated coastal area using statistics, GIS, and hydrogeochemical investigations. *Environ Sci Pollut* 22:2643–2660
- Brindha K, Pavelic P, Sotoukee T, Douangsavanh S, Elango L (2017) Geochemical characteristics and groundwater quality in the Vientiane Plain. *Laos Exposure Health* 9(2):89–104
- Chadda DK (1999) A proposed new diagram for geochemical classification of natural waters and interpretation of chemical data. *Hydrogeol J* 7(5):431–439. <https://doi.org/10.1007/s100400050216>
- Das N, Deka JP, Shim J, Patel AK, Kumar A, Sarma KP, Kumar M (2016) Effect of river proximity on the arsenic and fluoride distribution in the aquifers of the Brahmaputra Floodplains, Assam, Northeast India. *Groundw Sustain Dev* 2–3:130–142
- Demlie M, Hingston E, Mnisi Z (2014) A study of the sources, human health implications and low cost treatment options of iron rich groundwater in the northeastern coastal areas of Kwa-Zulu-Natal, South Africa. *J Geochem Explor* 144:504–510. <https://doi.org/10.1016/j.gexplo.2014.05.011>
- Di Curzio D, Palmucci W, Rusi S, Signanini P, (2017) Multidisciplinary approach to assess the seasonal effect on redox processes occurring in a tropical alluvial aquifer. In: *Proceedings of the 3rd National Meeting on Hydrogeology*, Cagliari, Italy, pp 11790–11805
- Duggal V, Rani A, Mehra R, Balaram V (2017) Risk assessment of metals from groundwater in northeast Rajasthan. *J Geol Soc India* 90(1):77–84
- Du Plessis A (2017) Freshwater Challenges of South Africa and its Upper Vaal River: current state and outlook. https://doi.org/10.1007/978-3-319-49502-6_4
- DWAF (Department of Water Affairs and Forestry) (1996) South African water quality guidelines (second edition). Volume 1: domestic use, In: D.o.W.A.a. (ed.), Forestry. Pretoria, p 214
- DWAF (Department of Water Affairs and Forestry) (2002) Water quality issues in the Usutu-Mhlathuze: review of water quality status and issues in the WMA. Prepared for DWAF/DFID Strategic Environmental Assessment by CPH Water (August), Pretoria. p 27
- Edokpayi JN, Enitan AM, Mutileni N, Odiyo JO (2018) Evaluation of water quality and human risk assessment due to heavy metals in groundwater around Muledane area of Vhembe District, Limpopo Province. *South Africa Chem Cent J* 12(1):1–16. <https://doi.org/10.1186/s13065-017-0369-y>
- Egbueri JC (2020) Heavy metals pollution source identification and probabilistic health risk assessment of shallow groundwater in Onitsha, Nigeria *Anal Lett*. <https://doi.org/10.1080/00032719.2020.1712606>
- Egbueri JC, Mgbenu CN (2020) Chemometric analysis for pollution source identification and human health risk assessment of water resources in Ojoto Province, southeast. *Appl Water Sci*. <https://doi.org/10.1007/s13201-020-01180-9>
- Eissa MA, Thomas JM, Pohll G, Shouakar-Stash O, Hershey RL, Dawoud M (2016) Groundwater recharge and salinization in the arid coastal plain aquifer of the Wadi Watir delta, Sinai. *Egypt Appl Geochem* 71:48–62
- Elango L, Kannan R, Senthil Kumar M (2003) Major ion chemistry and identification of hydrogeochemical processes of groundwater in a part of Kancheepuram district, Tamil Nadu, India.

- Environ. Geosci. 10(4): 157e166. <https://doi.org/10.1306/eg100403011>
- Esmaeili S, Asghari Moghaddam A, Barzegar R, Tziritis E (2018) Multivariate statistics and hydrogeochemical modeling for source identification of major elements and heavy metals in the groundwater of Qareh-Ziaeddin plain. NW Iran Arab J Geosci 11(1):1–14. <https://doi.org/10.1007/s12517-017-3317-1>
- Etikala B, Golla V, Adimalla N, Marapatla S (2019) Factors controlling groundwater chemistry of Renigunta area, Chittoor District, Andhra Pradesh, South India: a multivariate statistical approach. HydroResearch 1:57–62
- Freeze RA, Cherry JA (1979) Groundwater. Prentice Hall Inc, Englewood Cliffs
- Ghesquière O, Walter J, Chesnaux R, Rouleau A (2015) Scenarios of groundwater chemical evolution in a region of the Canadian Shield based on multivariate statistical analysis. J Hydrol Reg Stud 4:246–266
- Grundling AT, Berg ECVD, Price JS (2013) Assessing the distribution of wetlands over wet and dry periods and land-use change on the Maputaland Coastal Plain, north-eastern KwaZulu-Natal, South Africa. S Afr J Geomat 2:120–139. <https://sajg.org.za/index.php/sajg/article/view/84>
- He X, Li P (2020) Surface water pollution in the middle Chinese Loess Plateau with special focus on hexavalent chromium (Cr^{6+}): occurrence, sources and health risks. Expo Health. <https://doi.org/10.1007/s12403-020-00344-x>
- He X, Li P, Wu J, Wei M, Ren X, Wang D (2020) Poor groundwater quality and high potential health risks in the Datong Basin, northern China: research from published data. Environ Geochem Health. <https://doi.org/10.1007/s10653-020-00520-7>
- Iqbal J, Nazzal Y, Howari F, Xavier C, Yousef A (2018) Hydrochemical processes determining the groundwater quality for irrigation use in an arid environment: the case of Liwa Aquifer, Abu Dhabi, United Arab Emirates. Groundw Sustain Dev. <https://doi.org/10.1016/j.gsd.2018.06.004>
- Jahanshahi R, Zare M (2015) Assessment of heavy metals pollution in groundwater of Golgohar iron ore mine area. Iran Environ Earth Sci 74:505–520
- Ji Y, Wu J, Wang Y, Elumalai V, Subramani T (2020) Seasonal variation of drinking water quality and human health risk assessment in Hancheng City of Guanzhong Plain, China. Expo Health. <https://doi.org/10.1007/s12403-020-00357-6>
- Kanagaraj G, Elango L, Sridhar SGD, Gowrisankar G (2018) Hydrogeochemical processes and influence of seawater intrusion in coastal aquifers south of Chennai, Tamil Nadu, India. Environ Sci Pollut Res 25:8989–9011
- Karroum M, Elgettafi M, Elmandour A, Wilske C, Himi M, Casas A (2017) Geochemical processes controlling groundwater quality under semiarid environment: a case study in central Morocco. Sci Total Environ 609:1140–1151
- Kelbe BE, Grundling AT, Price JS (2016) Modelling water-table depth in a primary aquifer to identify potential wetland hydrogeomorphic settings on the northern Maputaland Coastal Plain, KwaZulu-Natal, South Africa. Hydrogeol J 24:249–265
- Kuldip S, Hundal HS, Dhanwinder S (2011) Geochemistry and assessment of hydrogeochemical processes in groundwater in the southern part of Bathinda district of Punjab, northwest India. Environ Earth Sci 64:1823–1833
- Li P, Li X, Meng X, Li M, Zhang Y (2016) Appraising groundwater quality and health risks from contamination in a semiarid region of northwest China. Expo Health 8(3):361–379. <https://doi.org/10.1007/s12403-016-0205-y>
- Li P, Feng W, Xue C, Tian R, Wang S (2017) Spatiotemporal variability of contaminants in lake water and their risks to human health: a case study of the Shahu Lake tourist area, northwest China. Expo Health 9(3):213–225. <https://doi.org/10.1007/s12403-016-0237-3>
- Li P, He X, Guo W (2019) Spatial groundwater quality and potential health risks due to nitrate ingestion through drinking water: a case study in Yan'an City on the Loess Plateau of northwest China. Hum Ecol Risk Assess 25(1–2):11–31. <https://doi.org/10.1080/10807039.2018.1553612>
- Mayback M (1987) Global chemical weathering of surficial rocks estimated from river dissolved loads. Am J Sci 287:401–428
- McMahon PB, Chapelle FH (2008) Redox processes and water quality of selected principal aquifer systems. Ground Water 46:259–271
- Meyer R, Talma AS, Duvenhage AWA, Eglington BM, Taljaard J, Botha JP, Verwey J, van der Voort I (2001) Geohydrological Investigation and Evaluation of the Zululand Coastal Aquifer. WRC Report No. 221/1/1. Pretoria. WRC
- Mkhwanazi MN (2010) Establishment of the Relationship Between the Sediments Mineral Composition and Groundwater Quality of the Primary Aquifers in the Maputaland Coastal Plain. Dissertation, University of Zululand
- Ndlovu M (2015) Hydrogeological conceptual modelling of the Kosi Bay lake system, North eastern South Africa. Dissertation, University of KwaZuluNatal
- Ndlovu M, Demlie M (2016) Hydrogeological characterization of the Kosi Bay Lakes system, north-eastern South Africa. Environ Earth Sci 75(19):1–16. <https://doi.org/10.1007/s12665-016-6164-6>
- Ndlovu MS, Demlie M (2018) Statistical analysis of groundwater level variability across KwaZulu-Natal Province. South Africa Environ Earth Sci 77(21):1–15. <https://doi.org/10.1007/s12665-018-7929-x>
- Nsubuga FNW, Mearns KF, Adeola AM (2019) Lake Sibayi variations in response to climate variability in northern KwaZulu-Natal, South Africa. Theor Appl Climatol 137:1233–1245
- Nweze A (2016) Characterization of the hydro stratigraphic units of the Sodwana Bay area using the electrical resistivity method. Dissertation, University of Zululand
- Palmucci W, Rusi S, Di Curzio D (2016) Mobilisation processes responsible for iron and manganese contamination of groundwater in Central Adriatic Italy. Environ Sci Pollut 23(12):11790–11805. <https://doi.org/10.1007/s11356-016-6371-4>
- Papazotos P, Koumantakis I, Vasileiou E (2019) Hydrogeochemical assessment and suitability of groundwater in a typical Mediterranean coastal area: a case study of the Marathon basin, NE Attica, Greece. HydroResearch 2:49–59
- Park SC, Yun ST, Chae GT, Yoo IS, Shin KS, Heo CH, Lee SK (2005) Regional hydrochemical study on salinization of coastal aquifers, western coastal area of South Korea. J Hydrol 313:182–194
- Paul R, Brindha K, Gowrisankar G, TanSingh MLMK (2019) Identification of hydrogeochemical processes controlling groundwater quality in Tripura, Northeast India using evaluation indices, GIS, and multivariate statistical methods. Environ Earth Sci 78:470
- Piper AM (1944) A graphic procedure in the geochemical interpretation of water analyses. Trans Am Geophys Union 25:914–928
- Porat N, Botha G (2008) The luminescence chronology of dune development on the Maputaland coastal plain, southeast Africa. Quarter Sci Rev 27:1024–1046
- Rajmohan N, Elango L (2004) Identification and evolution of hydrogeochemical processes in the groundwater environment in an area of the Palar and Cheyyar River Basins, Southern India. Environ Geol 46:47–61
- Revelle R (1941) Criteria for recognition of sea water in groundwaters. Trans Am Geophys Union 22:593–597
- Sawyer CN, McCarty PL (1978) Chemistry of environmental engineering. McGraw-Hill, New York

- Schoeller H (1965) Qualitative evaluation of groundwater resources. In: methods and techniques of groundwater investigations and development. In: Proceedings of the UNESCO, pp 54–83
- Seddique AA, Masuda H, Anma R, Bhattacharya P, Yokoo Y, Shimizu Y (2019) Hydrogeochemical and isotopic signatures for the identification of seawater intrusion in the paleobeach aquifer of Cox's Bazar city and its surrounding area, south-east Bangladesh. *Groundw Sustain Dev* 9:100215
- Sharma S, Bhattacharya A (2017) Drinking water contamination and treatment techniques. *Appl Water Sci* 7:1043–1067
- Smakhtin V, Ashton P, Batchelor A, Meyer R, Murray E, Barta B, Bauer N, Naidoo D, Olivier J, Terblanche D (2001) Unconventional water supply options in South Africa. *Water Int* 26:314–334
- Smithers J, Gray R, Johnson S, Still D (2017) Modelling and water yield assessment of Lake Sibhayi. *Water SA* 43:480–491
- Soleimani H, Azhdarpoor A, Hashemi H, Radfard M, Nasri O, Ghoochani M, Azizi H, Mahvi AH (2020) Probabilistic and deterministic approaches to estimation of non-carcinogenic human health risk due to heavy metals in groundwater resources of torbat heydariyeh, southeastern of Iran. *Int J Environ Anal Chem*. <https://doi.org/10.1080/03067319.2020.1757086>
- Soltani S, Asghari Moghaddam A, Barzegar R, Kazemian N, Tziritis E (2017) NW Iran: application of multivariate statistical analysis and PoS index. *Environ Monit Assess*. <https://doi.org/10.1007/s10661-017-6171-4>
- Stallard RF, Edmond JM (1983) Geochemistry of the Amazon: 2. The influence of geology and weathering environment on the dissolved load. *J Geophys Res* 88:9671–9688
- Still DA, Nash SR (2002) Groundwater contamination due to pit latrines located in a sandy aquifer a case study from Maputaland. In: Proceedings of the Water Institute of South Africa Biennial Conference, pp 1–6
- Tamasi G, Cini R (2004) Heavy metals in drinking waters from Mount Amiata (Tuscany, Italy). Possible risks from arsenic for public health in the Province of Siena. *Sci Total Environ* 327:41–51
- Tay CK, Hayford E (2016) Levels, source determination and health implications of trace metals in groundwater within the Lower Pra Basin. *Ghana Environ Earth Sci* 75(18):1–19. <https://doi.org/10.1007/s12665-016-6034-2>
- Telahigue F, Agoubi B, Souid F, Kharroubi A (2018) Assessment of seawater intrusion in an arid coastal aquifer, south-eastern Tunisia, using multivariate statistical analysis and chloride mass balance. *Phys Chem Earth, Parts A/B/C* 106:37–46
- Tiwari AK, Pisciotta A, De Maio M (2019) Evaluation of groundwater salinization and pollution level on Favignana Island, Italy. *Environ Pollut* 249:969–981
- Ukah BU, Egbueri JC, Unigwe CO, Ubido OE (2019) Extent of heavy metals pollution and health risk assessment of groundwater in a densely populated industrial area, Lagos, Nigeria. *Int J Energ Water Res*. <https://doi.org/10.1007/s42108-019-00039-3>
- Umarani P, Ramu A, Kumar V (2019) Hydrochemical and statistical evaluation of groundwater quality in coastal aquifers in Tamil Nadu. *India Environ Earth Sci* 78(15):1–14. <https://doi.org/10.1007/s12665-019-8414-x>
- USEPA (US Environmental Protection Agency (2004) Risk Assessment guidance for superfund volume, Human health evaluation manual (part E. Supplemental Guidance for Dermal risk assessment) EPA/540/R;99/005. Office of the superfund Remediation and Technology Innovation. U.S. Environmental Protection Agency, Washington, DC
- Usman UA, Yusoff I, Raooov M, Hodgkinson J (2020) Trace metals geochemistry for health assessment coupled with adsorption remediation method for the groundwater of Lorong Serai 4, Hulu Langat, west coast of Peninsular Malaysia. *Environ Geochem Health*. <https://doi.org/10.1007/s10653-020-00543-0>
- Verlicchi P (2020) Grillini V (2020) Surface water and groundwater quality in South Africa and Mozambique-analysis of the most critical pollutants for drinking purposes and challenges in water treatment selection. *Water* 12:305. <https://doi.org/10.3390/w12010305>
- Vetrimurugan E, Brindha K, Elango L (2017a) Human exposure risk assessment due to heavy metals in groundwater by pollution index and multivariate statistical methods: an application from South Africa. *Water* 9:234
- Vetrimurugan E, Brindha K, Elango L (2017b) Regional and temporal variation in minor ions in groundwater of a part of a large river delta, southern India. *Environ Monit Assess* 189(7):305
- Vetrimurugan E, Brindha K, Sithole B, Lakshmanan E (2017c) Spatial interpolation methods and geostatistics for mapping groundwater contamination in a coastal area. *Environ Sci Pollut Res* 24:11601–11617
- Vetrimurugan E, Dlamini PN, Natarajan R (2019) Evaluation of high fluoride contaminated fractured rock aquifer in South Africa—Geochemical and chemometric approaches. *Chemosphere*. <https://doi.org/10.1016/j.chemosphere.2019.06.065>
- Vetrimurugan E, Elango L, Rajmohan N (2013) Sources of contaminants and groundwater quality in the coastal part of a river delta. *Int J Environ Sci Technol* 10:473–486
- Vhonani GN, Vetrimurugan E, Rajmohan N (2018) Irrigation return flow induced mineral weathering and ion exchange reactions in the aquifer, Luvuvhu catchment, South Africa. *J Afr Earth Sci* 149:517–528
- Wagh VM, Panaskar DB, Mukate SV, Gaikwad SK, Muley AA, Varade AM (2018) Health risk assessment of heavy metal contamination in groundwater of Kadava River Basin, Nashik, India. *Model Earth Syst Environ* 4:969–980
- Wang H, Gu H, Lan S, Wang M, Chi B (2018) Human health risk assessment and sources analysis of nitrate in shallow groundwater of the Liujiang basin, China. *Hum Ecol Risk Assess* 24(6):1–17. <https://doi.org/10.1080/10807039.2017.1416455>
- Wang J, Liu GJ, Liu HQ, Lam PKS (2017) Multivariate statistical evaluation of dissolved trace elements and a water quality assessment in the middle reaches of Huaihe river, Anhui, China. *Sci Tot Environ* 583:421–431
- Watkeys MK, Mason TR, Goodman PS (1993) The rôle of geology in the development of Maputaland, South Africa. *J Afr Earth Sci* 16:205–221
- Weitz J, Demlie M (2014) Conceptual modelling of groundwater–surface water interactions in the Lake Sibayi Catchment, Eastern South Africa. *J Afr Earth Sci* 99:613–624
- WHO (1996) Health criteria and other supporting information. Guidelines for Drinking-Water Quality 2nd ed
- WHO (2011) Guidelines for drinking water quality, 4th edn. World Health Organization, Geneva
- Wu B, Zhao DY, Jia HY, Zhang Y, Zhang XX, Cheng SP (2009) Preliminary risk assessment of trace metal pollution in surface water from Yangtze River in Nanjing Section, China. *Bull Environ Contam Toxicol* 82(4):405–409
- Wu J, Zhou H, He S, Zhang Y (2019) Comprehensive understanding of groundwater quality for domestic and agricultural purposes in terms of health risks in a coal mine area of the Ordos basin, north of the Chinese Loess Plateau. *Environ Earth Sci* 78(15):446. <https://doi.org/10.1007/s12665-019-8471-1>
- Wu J, Zhang Y, Zhou H (2020) Groundwater chemistry and groundwater quality index incorporating health risk weighting in Dingbian County, Ordos basin of northwest China. *Geochemistry*. <https://doi.org/10.1016/j.chemer.2020.125607>
- Yohana M, Ibrahim CM, Charles B, Van Marc C, Kristine M, Kristine W (2013) Saltwater intrusion and nitrate pollution in the coastal aquifer of Dar es Salaam, Tanzania. *Environ Earth Sci* 70:1091–1111. <https://doi.org/10.1007/s12665-012-2197-7>

- Yousaf B, Amina Liu G, Wang R, Imtiaz M, Rizwan MS, Zia-Ur-Rehman M, Qadir A, Si Y (2016) The importance of evaluating metal exposure and predicting human health risks in urban-periurban environments influenced by emerging industry. *Chemosphere* 150:79–89
- Zaidi FK, Nazzal Y, Jafri MK, Naeem M, Ahmed I (2015) Reverse ion exchange as a major process controlling the groundwater chemistry in an arid environment: a case study from northwestern Saudi Arabia. *Environ Monit Assess* 187:607. <https://doi.org/10.1007/s10661-015-4828-4>
- Zeng XX, Liu YG, You SH, Zeng GM, Tan XF, Hu XJ, Hu X, Huang L, Li F (2015) Spatial distribution, health risk assessment and statistical source identification of the trace elements in surface water from the Xiangjiang River China. *Environ Sci Pollut Res* 22:9400–9412. <https://doi.org/10.1007/s11356-014-4064-4>
- Zhang Y, Wu J, Xu B (2018) Human health risk assessment of groundwater nitrogen pollution in Jinghui canal irrigation area of the loess region, northwest China. *Environ Earth Sci* 77:273. <https://doi.org/10.1007/s12665-018-7456-9>
- Zhou Y, Li P, Chen M, Dong Z, Lu C (2020) Groundwater quality for potable and irrigation uses and associated health risk in southern part of Gu'an County, North China Plain. *Environ Geochem Health*. <https://doi.org/10.1007/s10653-020-00553-y>
- Zhou Y, Wei A, Li J, Yan L, Li J (2016) Groundwater Quality Evaluation and Health Risk Assessment in the Yinchuan Region, northwest China. *Exposure Health* 8(3):443–456. <https://doi.org/10.1007/s12403-016-0219-5>

Publisher's Note Springer Nature remains neutral with regard to jurisdictional claims in published maps and institutional affiliations.